DYNAMIC CHARACTERISTICS AND RESPONSE OF A DOUBLE CANTILEVER BRIDGE

A Dissertation
submitted in partial fulfilment of
the requirements for the Degree of
MASTER OF ENGINEERING
in
EARTHQUAKE ENGINEERING
with specialisation in Structural Dynamics

By

PARSHURAM SINGH

SCHOOL OF RESEARCH AND TRAINING IN
EARTHQUAKE ENGINEERING,
UNIVERSITY OF ROORKEE
ROORKEE

June 1975

C E R T I F I C A T E

Certified that the thesis entitled "Dynamic Characteristics and response of a double cantilever bridge" which is being submitted by Shri Parshuram Singh in partial fulfilment for the award of the Degree of Master of Engineering in Earthquake Engineering with specialisation in Structural Dynamics is a record of student's own work carried out by him under our supervision and guidance. The matter embodied in this thesis has not been submitted for the award of any other degree or diploma.

This is further to certify that he has worked for a period of seven months from January 1974 to July 1974 for preparing this thesis for the Master of Engineering Degree at this University.

S. K. Thakkar

(S.K. Thakkar)
Reader in Structural Dynamics
Department of Earthquake Engineering
University of Roorkee
Roorkee

(A.S. Arya)
Professor and Head
Department of Earthquake Engineering
University of Roorkee
Roorkee

ACKNOWLEDGEMENT

The author expresses his sincere thanks to Dr. A.S. Arya, Professor and Head, and Dr. S.K. Thakkar, Reader in Structural Dynamics, Earthquake Engineering Department for encouragement, advice and guidance.

Thanks are also to the staff of Earthquake Engineering Workshop and Structural Dynamics Laboratory for their assistance in fabrication and testing of the model.

ABSTRACT

An experimental and analytical investigation has been carried out to determine the dynamic behaviour of a large span double cantilever reinforced concrete bridge. A perspex model of the bridge was prepared for the purpose of experimental and analytical investigation. The test program on the model includes static tests with horizontal loads applied near the top of well to determine its stiffness, free and steady state vibration tests on a shake table in longitudinal and transverse directions for both base fixed and bottom embedded in sand upto scour level conditions.

The dynamic analysis of the bridge has been carried out by Rayleigh's method. The masses were lumped along the well, pier and cantilever arms for dynamic analysis in the longitudinal direction but in the transverse direction entire superstructure was lumped at its centre of gravity.

First fundamental frequency in the longitudinal direction was found to be lower than that in the transverse direction. The ratio of horizontal acceleration along the height of substructure in the fixed base case was higher compared to the same when the model was embedded in sand. But in cantilever arm the ratio of vertical acceleration to the horizontal base acceleration was lower in the fixed

base case compared to the sand embedded case.

Dynamic moment in the cantilever arm of the prototype bridge even for a reduced displacement spectra of ElCentro earthquake of 1940, N-S component is nearly 11.3% of the dead load moment. Marked difference is seen in the dynamic response of the bridge in longitudinal and transverse directions.

TABLE OF CONTENTS

CHAPTER 1

INTRODUCTION

1.1 General

Indian Standard Code IS: 1893-1970 recommends the uniform seismic coefficient method of design for ordinary bridges. For special bridges dynamic analysis is recommended but it is being seldom resorted to by the designers. The double cantilever bridges have certain advantages over the usual simply supported T beam or balanced cantilever bridges. They are usually constructed with tall supporting structures and long cantilever arms. For such bridges dynamic analysis is expected to provide more rational basis for design.

In the present study a double cantilever highway bridge supported on a thick layer of uniform sand has been taken up for investigation. The length of cantilever arm is nearly equal to the height of substructure. Fig. 1.1 shows the sectional elevation of the bridge along the longitudinal centre line and the cross section of the well foundation. Fig. 1.2 shows the cross section of the bridge at the centre line of the pier. For the purpose of present investigation entire bridge has been considered to be built of reinforced concrete in concrete grade M 150.

It is likely that a very large and important bridge of this type to be built in thickly populated area, may need a minimum of four standard lanes. But paucity of funds may limit building only two lanes initially. As such in the present investigation both the stages of construction have been studied from dynamic point of view.

1.2 Brief Review of Literature

During the Bihar-Nepal Earthquake of 1934, not a bridge in the alluvial plain of north Bihar remained undamaged, from minor cracks in arches, wing walls and abutments, displaced piers and girders, to complete destruction[3]. Numerous examples of damages to permanent bridges during earthquakes all over the world are available[2]. These damages usually occur at intensity of VIII and above on Modified Mercalli Scale. Seismic damages are most commonly caused by foundation failures resulting from excessive ground deformation and/or loss of stability and bearing capacity of the foundation soils. As a direct result, the substructures often tilt, settle, slide, or even over turn; thus causing severe cracking or complete failure. These large support displacements also cause relative shifting of and damage to superstructures, induce failures within bearing supports, and even cause spans to fall off their supports. However examples of damages to superstructures of girder bridges directly as a result of structural vibration are few.

Most girder bridges in the past had vibration periods less than about 0.3 seconds and there was relatively little risk of resonance with earthquake motion[8]. With the advance of technology, bridge piers of girder bridges are becoming more and more flexible and the girder spans are increasing. As a result the natural period of vibration is becoming correspondingly longer and there is ample possibility of resonance with earthquake motion.

Structural vibrations are important for long span bridges with tall subsetures substructures. During San Fernando earthquake of February 9, 1971, numerous reinforced concrete highway bridges consisting of either straight or curved box girders of large span suffered severe damage as result of vibration[2].

During Fukui earthquake of June 28, 1948 (magnitude 7.3 on the Richter scale) superstructure of the Koroba bridge in Japan suffered large cracking near midspan of main girders in the first and second spans[1]. The superstructure had a total length of 36m and a width of 3.65m and consisted of three reinforced concrete T beams. Damage was obviously caused by vibrational effects of earthquake. Other instances of such damages have also come to light and have attracted the attention of investigators to this aspect of bridge design.

Elaborate dynamic analysis and model testing of a tied cantilever bridge was done by Krishna, Arya and Thakkar[5]. The well foundation of the bridge was 30.55 m high and the piers were 20.85 m tall. The cantilever arms on both sides of the pier were 72.10 m long. It was observed that tip of the cantilever suffered a large longitudinal displacement and acceleration at the top of pier during steady state test of the bridge model in longitudinal direction was 5.93 times the horizontal base acceleration. The dyanmic response obtained on the basis of dynamic analysis differed a great deal from that obtained by uniform seismic coefficient method. Thus it was considered that for a special structure like the tied cantilever bridge, dynamic analysis should be carried out to arrive at a rational design.

Dynamic characteristics of a large multispan reinforced concrete box girder bridge supported on and rigidly connected to the reinforced concrete columns and diaphragm abutments were studied by Tseng and Penzien[2]. Bridge was idealised by a discrete parameter system consisting of 71 nodal points located on the columns and girders. Foundation flexibilities were approximated by assuming the columns and abutments to be fully fixed at a depth of 10 ft below the ground surface. Under the earthquake of ElCentro 1940 NS Component, the maximum horizontal acceleration at the top of columns was 1.01 g and the maximum horizontal displacement at that point was found to be 1.45 ft. Charleson[6] measured the natural frequency and damping of a number of girder bridges built in New Zealand but his investigation was limited to the study of dynamic characteristics of substructures only.

However the dynamic characteristics of reinforced or prestrssed concrete bridge with long cantilever arms on both sides of the ~~subsetur~~ substructure has not been studied.

1.3 Objectives of Investigation

(i) To study the dynamic behaviour of the double cantilever bridge experimentally and analytically.

(ii) To compare the dynamic properties and amplification of acceleration of bridge model when it is fixed at the base to those when it is embedded in dry sand of predetermined density upto the assumed scour level.

(iii) To obtain the dynamic response of the prototype bridge for a typical earthquake motion.

1.4 Scope of the Thesis

A perspex model scaled down by a factor of 83.33 was prepared to study the dynamic behaviour of the bridge experimentally and analytically. The natural frequency, damping and dynamic amplification of the model in fixed base condition has been compared with those when the bottom of the well is embedded in dry sand below scour level.

Live loads on the deck of the bridge have not been taken into account and the section of the bridge has been assumed to be simple. The suspended span between well-pier-girder assemblage has been replaced by half of its dead weight at the end of the cantilever arm.

A certain quantity of water will vibrate along with the bridge, during earthquake motion but this has not been considered here because the effect of water can be found separately and the presence of water makes experimentation difficult. Since the shake table could be vibrated only in one direction, the model was turned in its shoe for vibration along the longitudinal and transverse axes. Vertical vibration of the bridge has not been considered.

Analytical investigation into the dynamic behaviour of the bridge model was carried out by Rayleigh's method lumping the masses along the body of the bridge at discrete points. With the help of analytical results of the model, dynamic response of the prototype under the spectral displacement of ElCentro May 18, 1940 N earthquake N-S component reduced to 0.349 times has been studied.

1.5 Notations

The letter symbols are defined wherever they appear first in the text. Important symbols are however given here in alphabetical order.

A	-	area of cross section of the well model
E_c	-	modulus of elasticity of concrete
E_m	-	modulus of elasticity of model material
E_p	-	modulus of elasticity of prototype

g - acceleration due to gravity

I - moment of inertia of the section

K - stiffness of the element

L - length of the element

m - mass of the element

n - scale ratio, the ratio of linear dimension of the prototype to the corresponding linear dimension of the model.

p - natural circular frequency of the dynamic system

T - time period of the vibrating system in seconds

- damping factor

- mass density of the material.

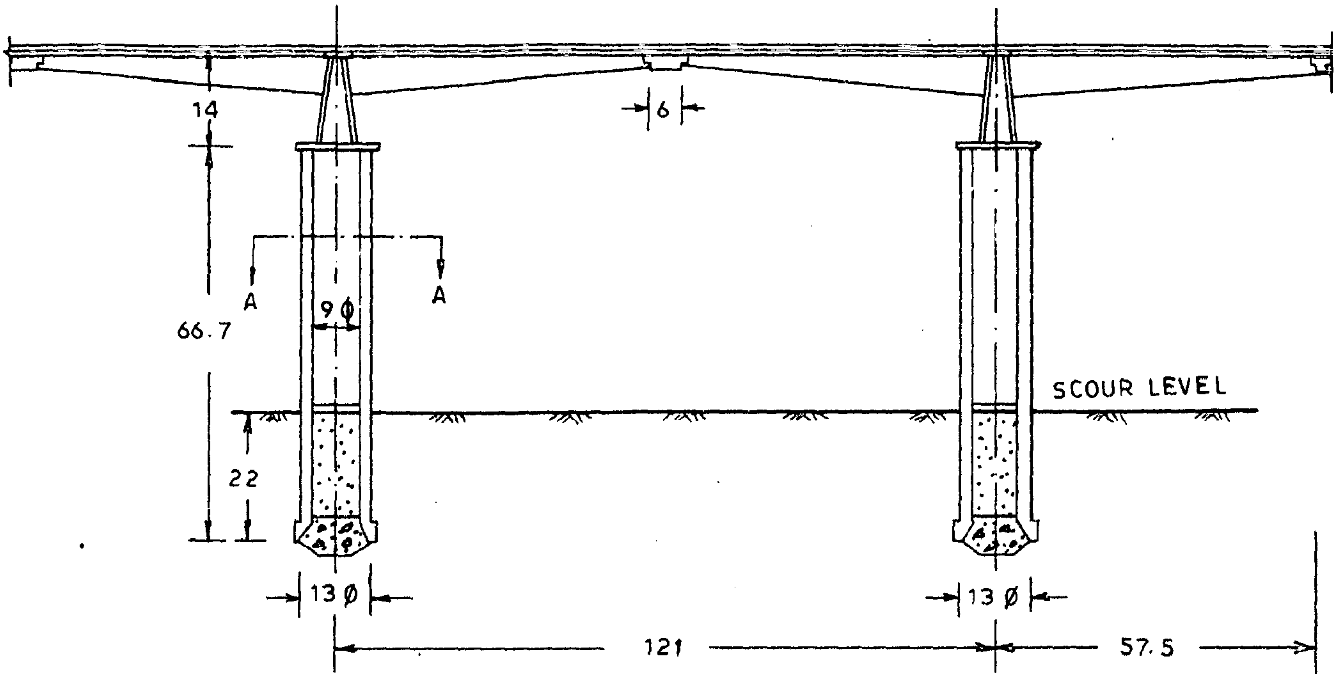

LONGITUDINAL SECTION OF THE BRIDGE

SCALE – 3/4 cm = 1 cm

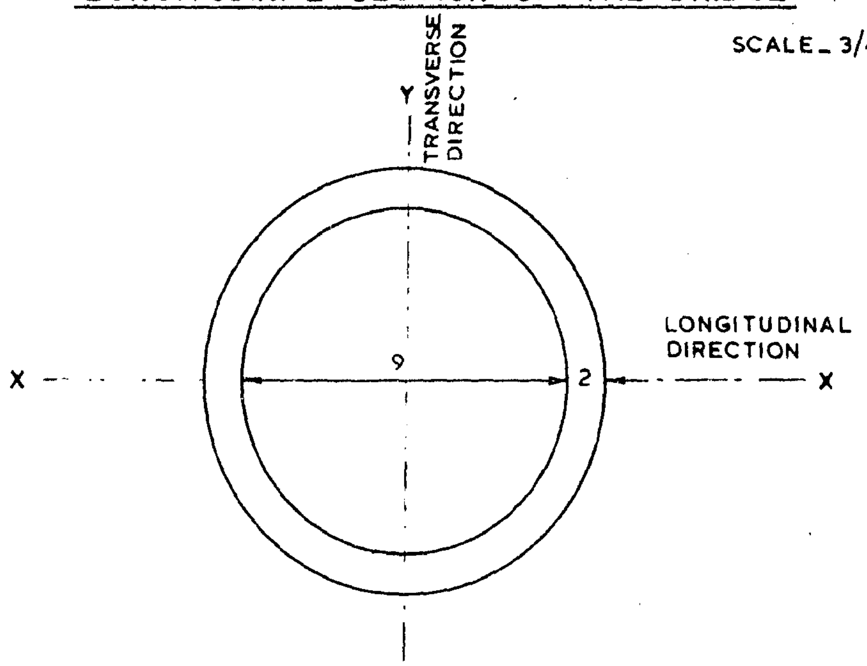

SECTION A.A.

SCALE 1 : 200

NOTE – 1. ALL DIMENSIONS IN m

2. CONCRETE GRADE M 150

FIG. 1.1

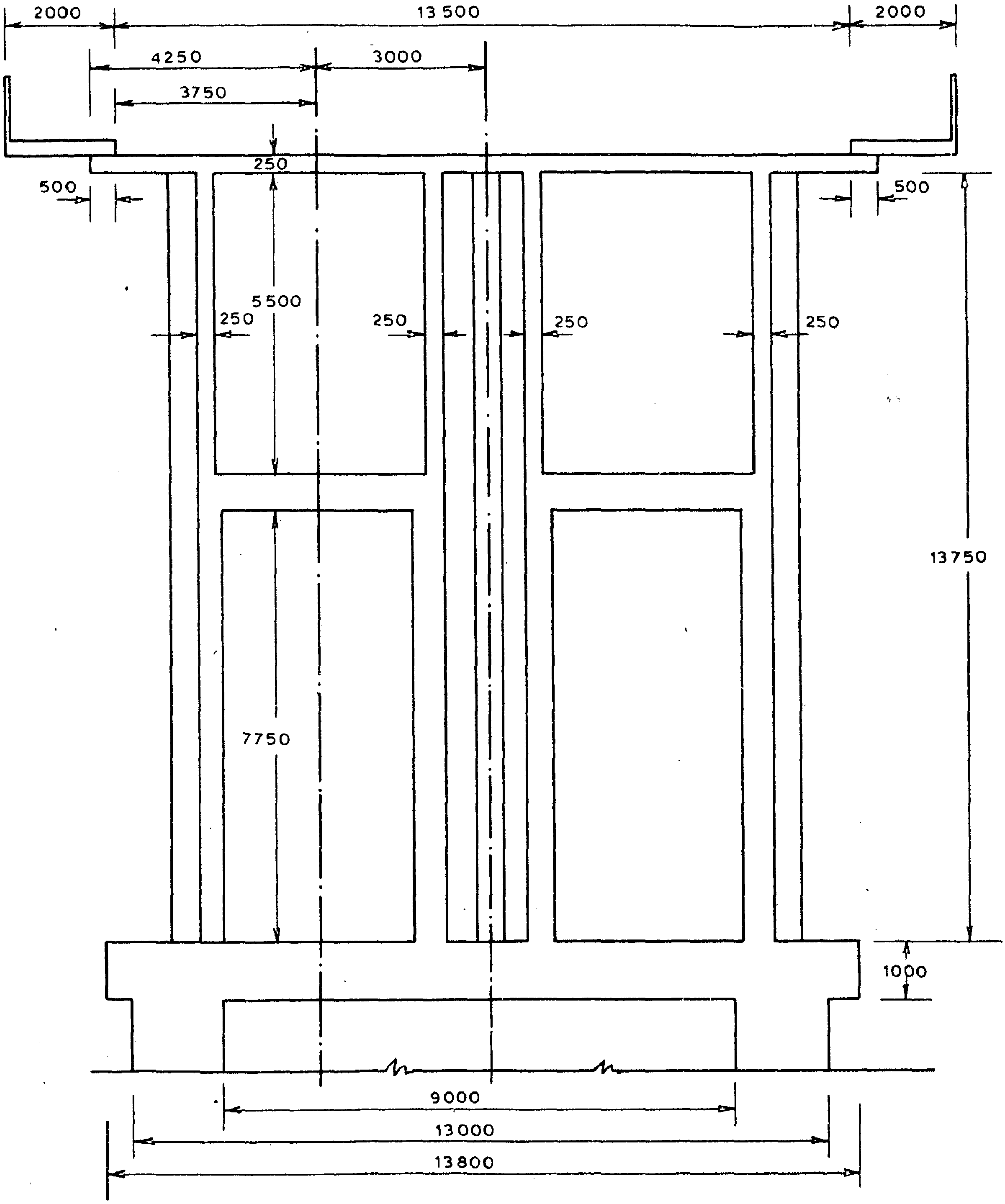

ALL DIMENSIONS IN mm

SCALE _ 1:100

SECTIONAL ELEVATION ALONG YY (PROTOTYPE BRIDGE)

FIG. 1·2

C H A P T E R 2

MODEL FOR INVESTIGATION

2.1 Scale Relation

$$\frac{\text{Stiffness of the prototype}}{\text{Stiffness of the model}} = \frac{K_p}{K_m} = \frac{E_p I_p}{(L_p)^3} \Big/ \frac{E_m I_m}{(L_m)^3}$$

and

$$\frac{m_p}{m_m} = \frac{\rho_p A_p L_p}{\rho_m A_m L_m} = n^3 \quad ; \quad p^2 = \frac{K}{m}$$

where,

K = bending stiffness

E = modulus of elasticity

I = moment of inertia

L = length of element

ρ = mass density of material

m = mass of the material

p = natural circular frequency

(Subscript p refers to the prototype and m to the model)

From above it can be deduced that

$$\frac{p_p}{p_m} = \frac{1}{n} \sqrt{\frac{E_p}{E_m} \frac{\rho_m}{\rho_p}}$$

n being the scale ratio.

2.2 Choice of the Model Material

For reinforced concrete girder bridges the Japanese Code 'Specification for Earthquake Resistant Design of Highway Bridges, Japan Road Association, January 1971 gives the following approximate formula for fundamental time period

$$T = 2\pi \sqrt{\frac{.3W_p + W_u}{3\ EIg} .h^3}$$

where

W_p = weight of the pier, tonnes

W_u = weight of the superstructure supported by the substructure, t

EI = flexural rigidity, tm^2

g = acceleration due to gravity, m/sec^2

h = height of pier , m

In the present case of prototype bridge

W_u = 3528 t

W_p = 11000 t

h = 75.5 m from the base to the underside of the girder

Assuming that the concrete in girder, pier and well is of grade M 150, for which E = 1125,000 t/m^2, and $I = 1000\ m^4$

$$T = 1.86 \text{ secs}$$

$$p_p = \frac{1}{1.86} = 0.54 \text{ cps}$$

Now come to limitations of testing:-

1. Dimension of the shake table was such that the length of model could not exceed 1.4 m
2. The forcing frequency with the available equipments could not exceed 40 cps

Since $$n = \sqrt{\frac{E_p \rho_m}{E_m \rho_p}} \times \frac{p_m}{p_n}$$

keeping $p_m = 40$ cps

$$n = \frac{40}{.54} \sqrt{\frac{E_p \rho_m}{E_m \rho_p}} = 74 \sqrt{\frac{E_p \rho_m}{E_m \rho_p}}$$

Keeping fabrication in view, steel cement-sand-mortar and perspex alone were considered and values of n were found to be 31,74 and 96 respectively. As such it was found that a length larger than permissible was required for steel whereas casting uniform sections as thin as 3 mm with cement sand mortar was impracticable; therefore the choice narrowed down to perspex. Besides, perspex has several advantages over other model materials. It exhibits linear stress strain relationship in the usual range of strains used in the models and the modulus of elasticity is quite low so that measurable strains and deflections can be obtained without requiring large loads or significant changes in geometry. It can be machined using the ordinary equipments of a machine shop with occasional slight modification.

2.3 Choice of Scale

Since the smallest thickness in the prototype was 250 mm and the perspex sheets were available in thicknesses of 3mm, 6 mm and 12 mm, a scale ratio of 250:3 from prototype to model was adopted. This scale gave the length of bridge model as 1390 mm which could be conveniently accommodated on the shake table. An equivalent octagonal cross section of the well was chosen in-stead of circular for a convenience of fabrication and testing .

2.4 Properties of the Model Material

To determine the modulus of elasticity of perspex, two specimens, each approximately 40 mm wide and 400 mm long from 6 mm and 12 mm sheets were cut out. Beam tests were performed and the results are shown in tables 2.1 and 2.2.

TABLE 2.1

DEFLECTION OF BEAM SPECIMEN (7 mm THICK)
UNDER POINT LOAD

Sl. No.	LOADING			UNLOADING		
	Load on pan gm	Dial reading (mm)	Deflection (mm)	Load on pan gm	Dial reading	Deflection (mm)
1	Initial	608	-	800	448	-
2	200	577	.26	600	475	.27
3	400	535	.73	400	517	.69
4	600	490	1.18	200	557	1.09
5	800	448	1.60	Pan + wire	600	1.52

TABLE 2.2

DEFLECTION OF BEAM SPECIMEN (13 mm THICK)
UNDER POINT LOAD

Sl. No.	LOADING			UNLOADING		
	Load on pan gm	Dial reading	Deflec-tion (mm)	Load on pan gm	Dial reading	Deflection (mm)
1	Initial	851	-	1500	801	-
2	500	840	.11	1000	808	.07
3	1000	820	.31	500	833	.32
4	1500	801	.50	Initial	855	.54

Fig. 2.1(a) and (b) show the variation of deflection against the applied load.

ELASTIC MODULUS OF PERSPEX FROM BEAM TESTS

Beam data	Beam (a)	Beam (b)
Width	40 mm	39 mm
Depth	7 mm	13 mm

Distance between supports 308 mm

Distance of point load from left hand support = 150 mm

Distance of dial gauge point from left hand support = 158 mm

Least count of dial gauge = .01 mm

Modulus elasticity of perspex from test on beam (a)

= 23200 kg/cm²

Modulus elasticity of perspex from test on beam (b)

= 22000 kg/cm²

Average value of modulus elasticity = 22600 kg/cm²

The weight density of the perspex was found to be 1.2 gm/cc and Poisson's ratio was taken to be 0.36[12].

2.5 Method of Fabrication

Girders and piers were fabricated from pieces of appropriate sizes cut from sheets of 3 mm and 6 mm thicknesses. The joinigg edges of the pieces were machined and polished smoorth so that no air bubbles were left when joined by chloroform.

The wall thickness of octagonal well was 24 mm whereas the thickest sheet avaialbe was only 12mm. So sixteen pieces were cut and joined giving eight pieces of 24 mm thickness. For this special care had to be taken so that chloroform reached all the places and no air bubbles were left. After the pieces to be joined were placed face to face, three sides were sealed with adhesive tapes and chloroform was injected through one of the sides, usually a long one. After the fluid reached all over the joining surface, the pieces were pressed hard by clamps so that extra fluid and air bubbles were ejected. Then they were machined to accurate sizes and angles. After polishing the edges of all the eight pieces, they were carefully joined to form a well 800 mm long and having the eross section shown in Fig. 2.2. The girders were joined to the piers first and then they were joined to the cap. Fig. 2.2 shows the longitudinal section of the model of the bridge, sectional plan of the piers and the cross section of the octagonal well. Cross sections of the girders of 2 Lane bridge and 4 Lane bridge are shown in Fig. 2.3.

After testing the well alone statically and dynamically, and getting satisfied that the well behaved as if it was of monolithic construction, it was joined to the well cap, pier and girder assembly. In the first stage only two lane bridge was prepared and after completion of all the tests on it, the remaining parts were connected to form the complete bridge carrying four lanes.

At various locations, holes were drilled and threads cut so that acceleration pickups could be attached to the model. Fig 2.4 shows the pick up location on the model in the longitudinal and transverse directions. A shoe of octagonal shape was made from steel angles 40 mm x 40 mm x 6 mm welded to a plate 300 mm x 300 mm x 12 mm thick to provide a fixed base to the model. Corrugated aluminium strips were placed between the faces of the well and shoe angles and the well was tightened by bolts.

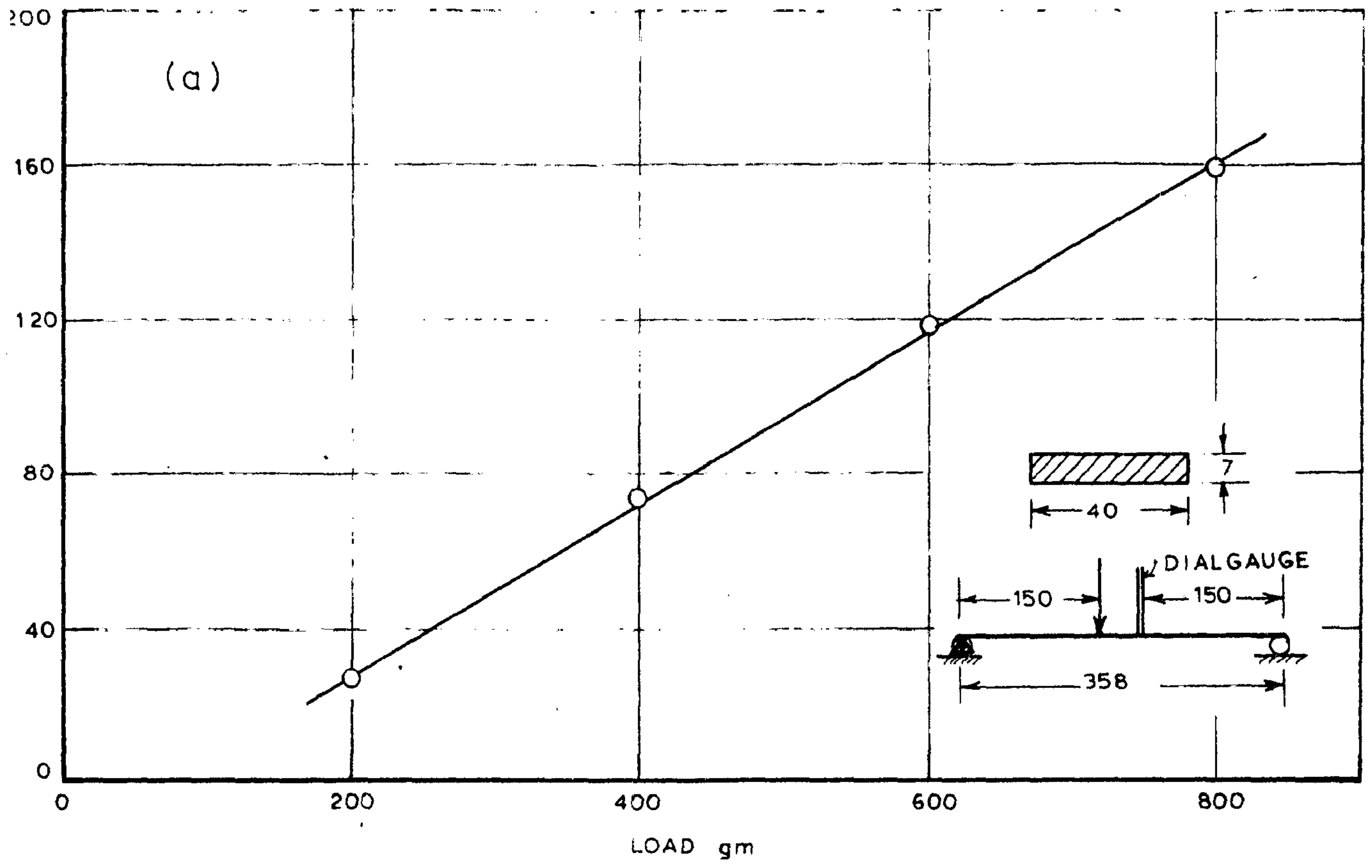

LOAD DEFLECTION DIAGRAM FOR 7 mm THICK BEAM SPECIMEN

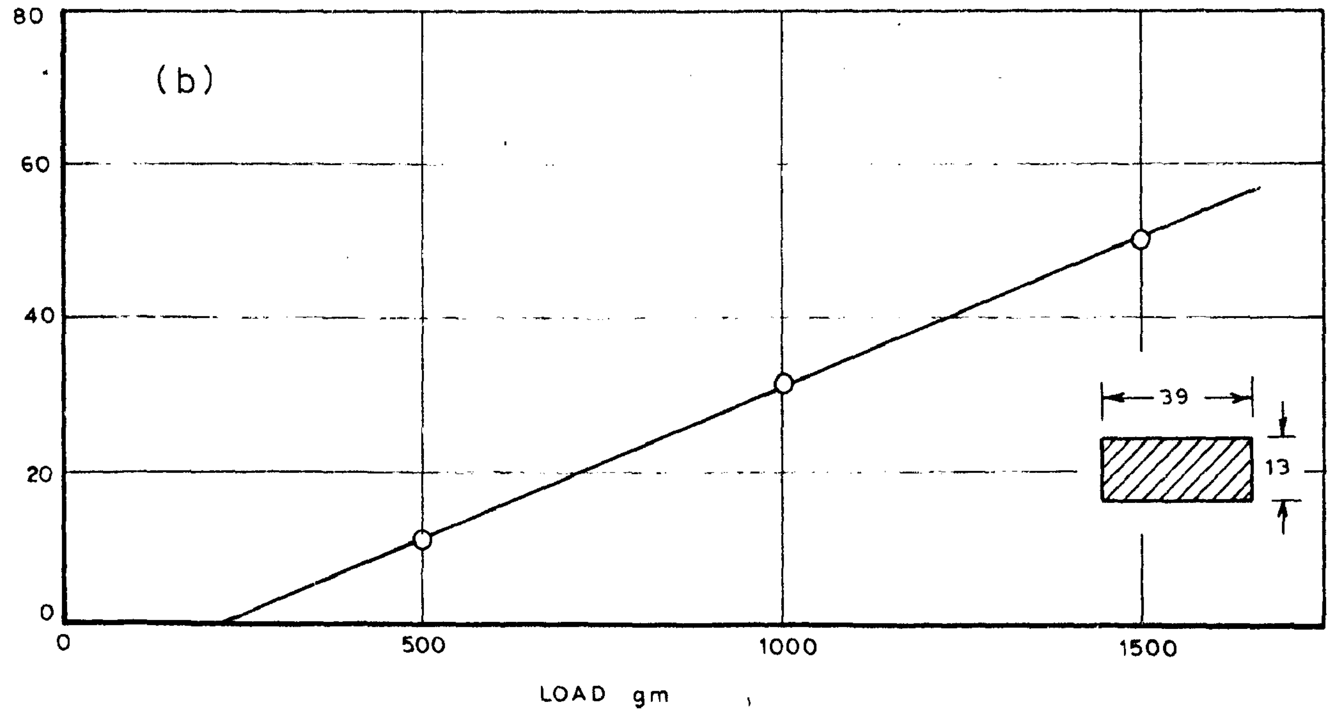

LOAD DEFLECTION DIAGRAM FOR 13 mm THICK BEAM SPECIMEN

FIG. 2.1

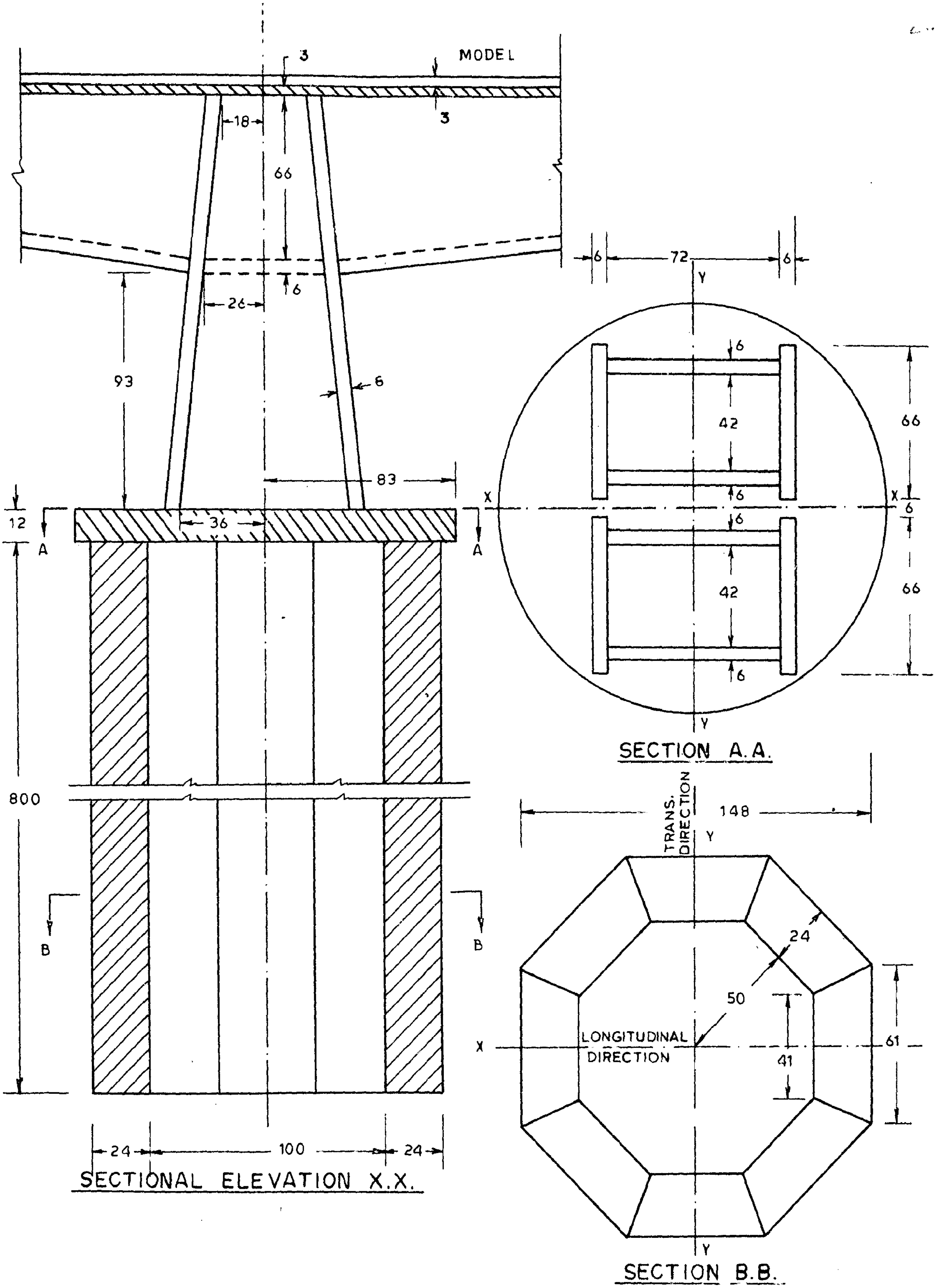

DIMENSIONS IN m. m.

FIG. 2.2 _ DETAILS OF PERSPEX MODEL OF BRIDGE

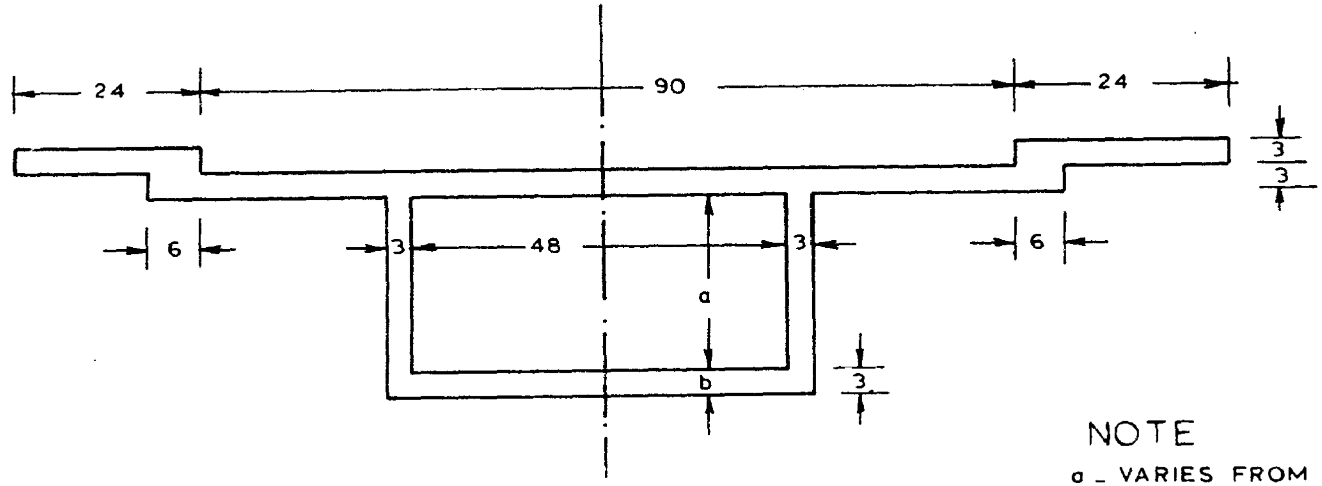

2-LANE BRIDGE MODEL

NOTE

a _ VARIES FROM 3mm AT THE TIP TO 6mm AT JUNCTION WITH PIER

b _ VARIES FROM 24 mm AT THE TIP TO 66mm AT JUNCTION WITH PIER

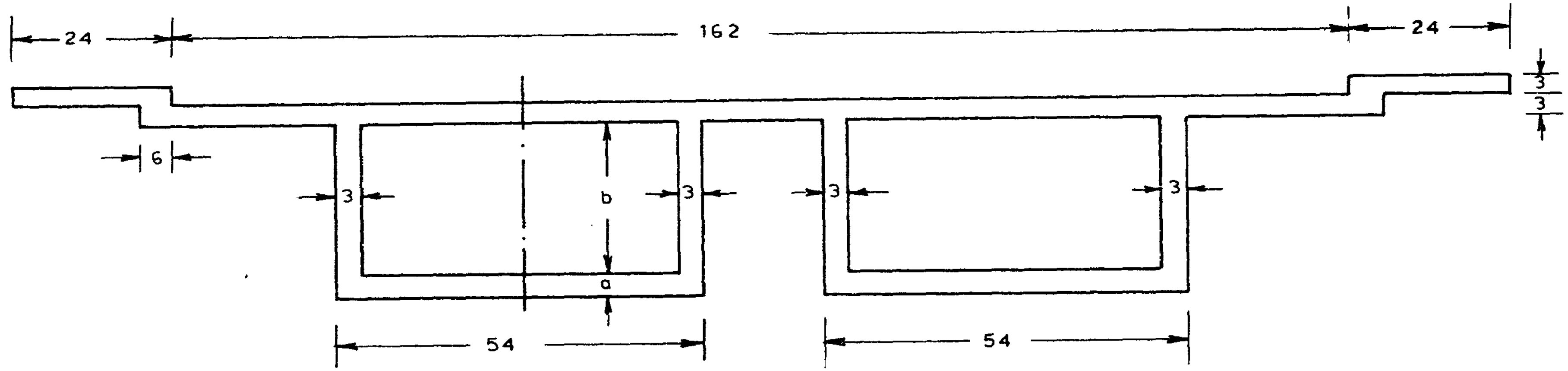

4-LANE BRIDGE MODEL

ALL DIMENSIONS IN mm

FIG. 2.3 _CROSS SECTION OF SUPERSTRUCTURE

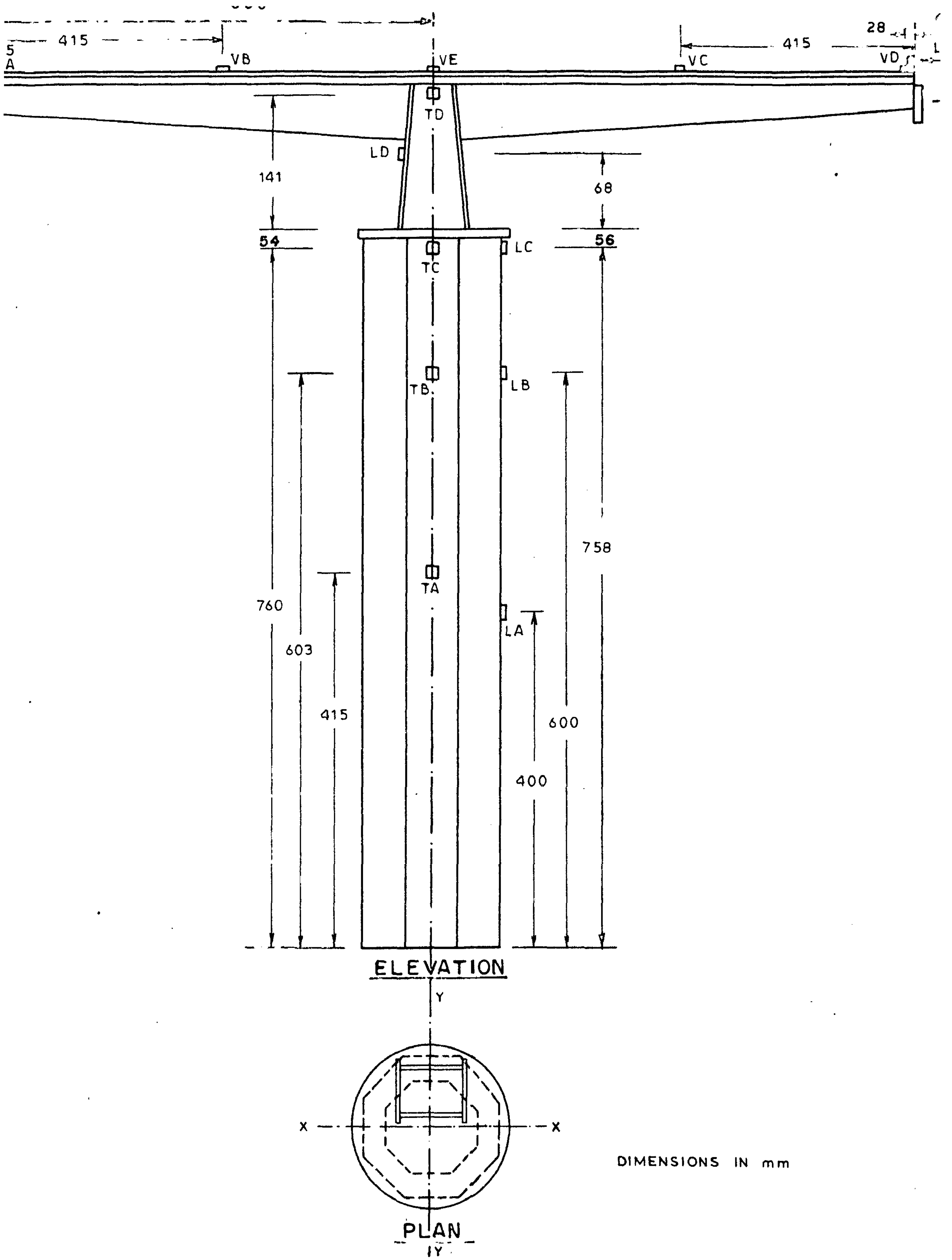

FIG. 2.4 _ PICK UP LOCATION ON MODEL

CHAPTER 3

TESTING PROGRAMME AND RESULTS

3.1 Types of Vibration Tests

Two types of vibration tests were conducted on the bridge model under each base condition - the free vibration tests and the steady state tests. For first the model was given a light jerk in the horizontal direction at the top. The acceleration at desired locations were recorded by acceleration pick-ups connected to pen recorders through amplifiers. For steady state tests a Lazan Oscillator was mounted on the shake table. The amplitude of vibration was adjusted by varying eccentricity of the knob and the frequency was changed by varying the resistance in the power supply unit.

3.2 Arrangement for Different Tests

For fixing the model at the base, a base plate was prepared wherein eight pieces of angles (40 x 40 x 6) were welded. Corrugated aluminium packing strips were placed between the model and the angles and the strips were then pressed to the surface of the model by means of bolts. The base plate was then secured to the shake table by means of 20 mm diameter bolts. For applying horizontal load at the top of the well, a thin aluminium strip 20 mm wide was fixed round the octagonal well and a flexible wire was connected to its end as shown in Fig. 3.1. Wire went round a frictionless pulley and weights of different denominations were placed on a pan connected to it at the end. Fixity at the base was checked by applying horizontal load at the top and measuring the resulting deflections and then comparing them with analytical results.

It was found from laboratory tests that the maximum density of the available sand was 1.68 gms/cc. Mark at 150 mm height was made on the side of the table. Sand required for filling a depth of 150 mm was weighed and poured in the tank. The top surface was made level. The knob of the oscillator attached to the table was kept at maximum eccentricity and the table was vibrated for about 90 seconds, by which time the top surface came to the level of the mark. The model was inverted and sand was poured to a height of 264 mm and the bottom of well was closed with a cap. The model was then placed on the sand bed in appropriate position and direction. Subsequent layers of sand were weighed, poured and vibrated inthe same way. Thus the model was embedded in dry sand of required density. Fig. 3.2 shows the bridge model on the shake table. The base is shown embedded in sand. A pick up and recording arrangements are shown in the back ground. For changing the direction of the model the entire process was repeated.

Since there were only three pick-ups available and one had to be attached to the base of the shake table, the whole range of tests with model in one particular direction had to be repeated a number of times to record accelerations at all the desired locations. Pick-ups were calibrated before and after each set of experiments.

3.3 Experimental Results

(a) Static Tests

(i) Static test on well alone fixed at the base

Stiffness of the well model having fixed base with respect to horizontal load applied and horizontal deflection measured at 10 mm below the top of the well wad determined by this test. Table 3.1 and 3.2 give the horizontal deflection at 10mm below the top of the well against horizontal load applied at that point.

TABLE 3.1

DEFLECTION OF WELL DUE TO HORIZONTAL LOAD ALONG XX AXIS (FIG. 2.2)

Load on pan (kg)	Dial gauge 1		Dial gauge 2		Dial gauge 3	
	Dial reading	deflection mm	Dial reading	deflec-tion mm	Dial reading	deflec-tion mm
Pan itself	098	-	100	-	09	0
2.275	86.5	.115	96.0	.04	09	0
4.550	74.5	.235	92	.08	09	0
5.550	69.0	.28	90	.10	09	0
6.550	63.5	.335	88	.12	09	0

TABLE 3.2

DEFLECTION OF WELL DUE TO HORIZONTAL LOAD ALONG YY AXIS (FIG. 2.2)

Load on Pan (kg)	LOADING		UNLOADING	
	Dial reading	Deflection mm	Dial reading	Declection mm
Initial	93	-	90	-
4.760	70	.23	65	.25
7.035	57.5	.355	53.0	.37
9.310	46.0	.47	43.0	.47
11.310	35.0	.58	35.0	.55

Note: Fig. 3.1 shows the test set up and the position of dial gauges.

The load deflection diagram has been plotted in Fig.3.3. The average of the stiffnesses in two direction was found to be 19.4 kg/mm.

(ii) Static test on the well model attached with the cap.

This test was conducted to see if there was any change in the stiffness of the well due to the attachment of the cap. The load was applied again horizontally at 10 mm below the top of well and horizontal deflection was measured at the same point. Table 3.3 and 3.4 give the deflection in mm against the applied load and deflection against load diagram has been plotted in Fig. 3.3.

TABLE 3.3

LOAD DEFLECTION TEST OF WELL WITH CAP

Load along XX axis (Fig.2.2)

Load on Pan (kg)	LOADING		UNLOADING	
	Dial reading	deflection mm	Dial reading	deflection mm
Initial	991	-	570	-
2.275	905	.86	653	83
4.550	800	1.91	760	1.90
6.825	680	3.11	860	2.90
9.100	570	4.21	960	3.90

TABLE 3.4

LOAD DEFLECTION TEST ON WELL WITH CAP
Load along yy axis (Fig.2.2)

Load on Pan (kg)	LOADING		UNLOADING	
	Dial reading	deflection mm	Dial reading	deflection mm
Initial	871	-	870	-
2.275	820	.51	790	.80
4.55	716	1.55	686	1.84
6.825	608	2.63	582	2.88
9.100	500	3.71	500	3.70

Note : Fig. 31 shows the test set up and the position of dial gauge.

The average of stiffnesses in longitudinal and transverse direction in this case was found to be 21.0 kg/mm.

(iii) Static test on the bridge model with two lanes of superstructure having the base embedded in dry sand upto scour level.

Horizontal load was applied at the top of well by means of a thin wire going over a frictionless pulley attached to the edge of the shake table. The deflection against the corresponding horizontal load is given in Table 3.5

TABLE 3.5

DEFLECTION NEAR TOP OF WELL AGAINST HORIZONTAL LOAD APPLIED ON THE 2 LANE BRIDGE MODEL EMBEDDED IN SAND UPTO SCOUR LEVEL

Load on Pan Kg	Dial reading	Deflection mm
Initial	648	-
2	635	.13
4	602	.46
6	563	1.05
8	488	1.63
10	100	5.48

The load deflection diagram has been plotted in Fig. 3.4

(b) Free Vibration Tests

(i) Free vibration test of well alone having fixed base

After fixing the well model at the base a light jerk was given to it near the top. Fig.3.6 shows the type of curve traced by the pen recorder. Natural frequency in the longitudinal direction (XX direction) was found to be 55.5 cps and the damping factor was .07. In the transverse direction (YY direction) also the natural frequency was 55.5 cps but the damping factor was .095.

(ii) Free vibration test of the 2-Lane bridge having fixed base.

A light jerk was given to the model at the end of the cantilever arm for excitation in the longitudinal direction and on the web of the girder above the pier for excitation in the transverse direction. Fig. 3.5 shows the curve generated by the free vibrations. In the longitudinal direction the natural frequency was found to be 35 cps and damping factor was .06 in the transverse direction they were 28 cps and .08 respectively.

(iii) Free vibration tests of 2-lane bridge having base embedded in sand upto a depth of 264 mm.

Fig. 3.5 shows the free vibration record in the longitudinal and transverse direction. The natural frequency and damping were found to be 38.5 cps and .07 respectively in the longitudinal direction while in the transverse direction they were 22.8 cps and .08 respectively.

(iv) The free vibration test of the 4-lane bridge having fixed base.

The model was excited by tapping the end of the cantilever arm. Fig. 3.6 shows the curve generated by the pen recorder. The natural frequency of vibration in the longitudinal direction was 21.2 cps and damping factor 0.08 while in the transverse direction they were 28 cps and .06 respectively.

(v) The free vibration test of 4-lane bridge having dry sand of density 1.68 gm/cc at the base upto a depth of 264 mm.

The model was excited in the longitudinal and transverse directions by giving light jerks at the vertical end of the girder. for excitation in the longitudinal direction. In the transfer direction the model was tapped at the top of the girder above the pier. Free vibration records are shown in Fig. 3.6. Natural frequency and damping factor in the longitudinal direction were found to be 20 cps and .08 and in the transverse direction they were 27 cps and .108 respectively.

(c) Steady State Tests

(i) Steady state test of 2-lane bridge model having fixed base.

Fig. 3.7 shows the relation between the ratio of acceleration at different points of the bridge to horizontal base acceleration and the forcing frequency. From the curves it is seen that first resonant frequency is nearly 21 cps and the second one 35 cps. Horizontal acceleration imparted at the base of the model is magnified to nearly four times near the top of substructure. The vertical acceleration at the tip of cantilever becomes almost 7 times the horizontal base acceleration at the moment of resonance.

In the transverse direction only one resonant frequency is recognisable in the range of forcing frequency possible with the available equipments. Response curve is shown in Fig. 3.10. The resonant frequency in this direction is seen to be 27 cps. Acceleration at the top of the pier was nearly twenty time that at the base. Even at the top of the well the acceleration was magnified nearly 7 times.

(ii) Steady state test of two lane bridge model having base embedded in dry sand upto a depth of 264 mm.

Resonance curves for vibration in are shown in figure 3.9. Here too, two resonant frequencies are easily seen in the longitudinal direction. The first resonant frequency is 23 cps and the second one is about 33 cps. In this case the acceleration near the top of the bridge is seen to be approximately 3 times the base acceleration and the variation along the height is almost linear. However acceleration magnification everywhere on the substructure is less compared to the fixed base case. On the cantilever arm the vertical acceleration is magnified to nearly nine times the base acceleration.

In the transverse direction the resonant frequency is seen to be nearly 27 cps and there is no other resonant frequency in the experimental range. Horizontal acceleration at the top of the poer is nearly seven times of that at the base but at the top of well the ratio reduces to nearly 3.

(iii) Steady state test of the 4-lane bridge model having fixed base

Resonance curves in Fig. 3.11 shows that the first resonant frequeny is nearly 22 cps. Horizontal acceleration at the top of well is approximately 3 times that at the base and the variation along the height is linear but above that the acceleration is seen to be nearly constant. In the cantilever arm, the ratio of vertical acceleration to the horizontal acceleration at the base is nearly 3.5.

In the transverse direction the first resonant frequency is seen to be as low as 17. However the horizontal acceleration is magnified nearly six times at the top of the well and the variation along the height is linear.

(iv) Steady state test of the 4-lane bridge model having base in dry sand upto 264 mm.

The first natural frequency is seen to be 21 cps and no other resonant frequency could be seen. Horizontal at the top of the girder is nearly twice that at the base and the variation is nearly linear along the height. In the cantilever arm the ratio of vertical acceleration to the horizontal base acceleration reached a value of nearly 7 near the tip of the cantilever.

In the transverse direction the first resonant frequency is nearly 23 cps. The ratio of horizontal acceleration at the top of well to that at the base is nearly 3 and the variation along the height is linear.

3.4 Interpretation of Experimental Results

(a) Static Tests

Stiffness of the well in two perpendicular directions was the same indicating that the pieces were joined well so that it behaved as if it was monolitic. Attachment of the cap to the well increased the stiffness of the well. The load deflection diagram is linear which means that the structure behaved elastically. But in the case of sand the load deflection diagram as shown in Fig. 3.4 is nonlinear right from the start and the resistance provided by sand almost vanishes at a very small load.

(b) Free Vibration Tests

Natural frequency of the well is seen to be the same in two perpendicular directions but the damping differs. This difference may be accounted to the fact that the frequency is high and measurements cannot be done accurately.

Natural frequency in the longitudinal direction for two lane bridge was higher than that in the transverse direction. Apparently the natural frequency registered was not the fundamental one. But in case of the complete bridge natural frequency in the longitudinal direction was lower. Damping varied from 6 to 10 %. Not much difference was seen between the fixed base case and base embedded in sand case.as regards natural frequency and damping.

(c) Steady State Tests

The first resonant frequency in the longitudinal direction is seen to be lower than that in the transverse direction. This indicated that the cantilever arms influenced the dynamic properties appreciably. Ratio of horizontal acceleration at the top of the pier to that at the base is more in the transverse direction. Ratio of vertical acceleration at the tip of the cantilever to the base acceleration is higher in two lane bridge. Dynamic properties of the bridge fixed at the base are very close to those when it is embedded in sand upto scour level.

The gist of the results of dynamic tests is given below in Table 3.6.

TABLE 3.6

DYNAMIC PROPERTIES OF THE BRIDGE MODEL FROM EXPERIMENTS

Description	Free Vibration Tests		Steady State Test		
	Natural frequency c/s	Damping	Resonant frequency c/s	Accele-ration ratio at top of pier	Accele-ration ratio at tip of cantilever
2 lane base bridge -fixed base					
Long.	35.0	.06	21.35	4	7
Trans.	28.0	.08	27	20	-
2 lane bridge base in sand					
Long.	38.5	.07	23.33	3	9
Trans.	22.8	.08	27	7	-
4-lane bridge base fixed					
Long.	21.2	.08	22	3	3.5
Trans.	29	.06	17	6	-
4-lane bridge base in sand					
Long.	20	.08	21	2	7
Trans.	27	.108	23	3	-

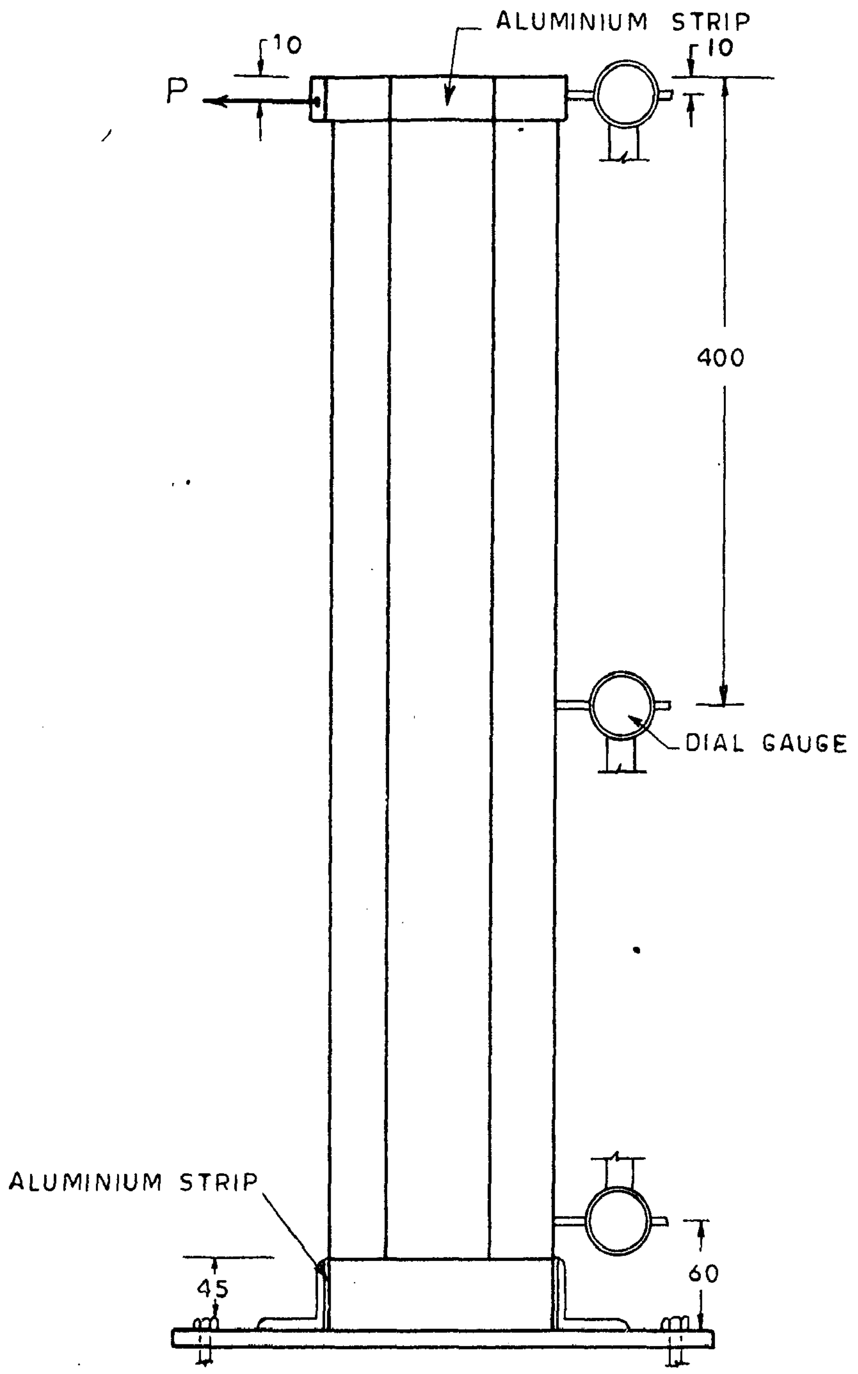

SCALE _ 1:5

FIG. 3.1 _ STATIC LOAD SET UP FOR WELL MODEL

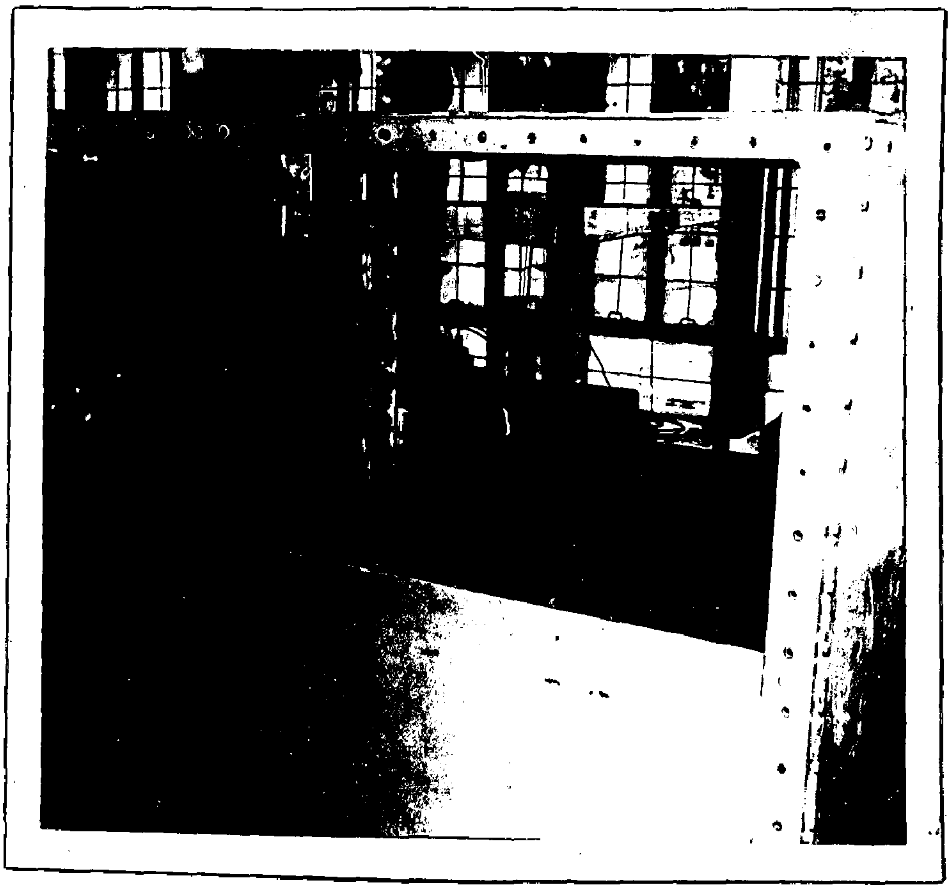

Fig 2.

ARRANGEMENT FOR RECORDING VIBRATION

ON BRIDGE MODEL

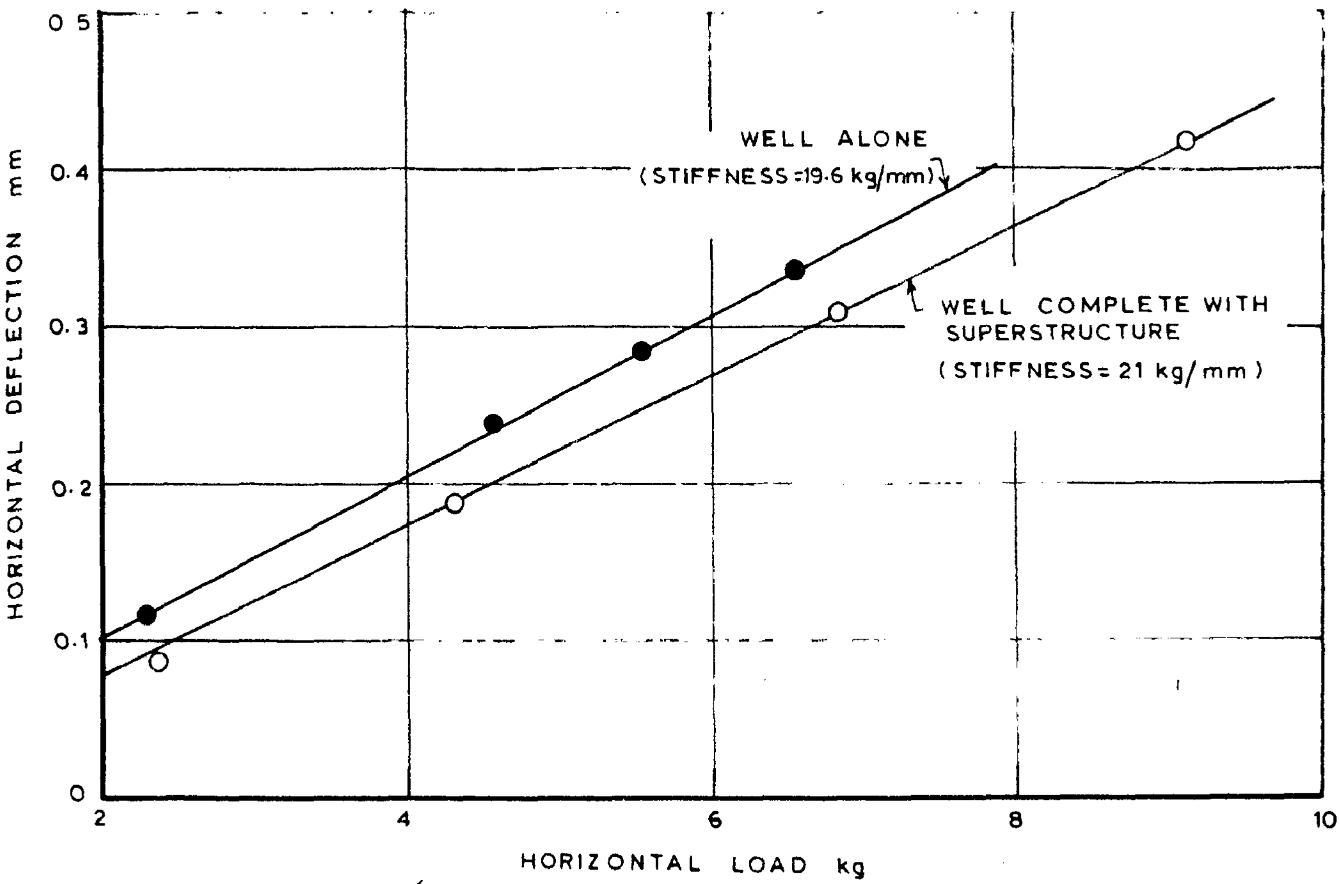

LOAD ALONG XX AXIS

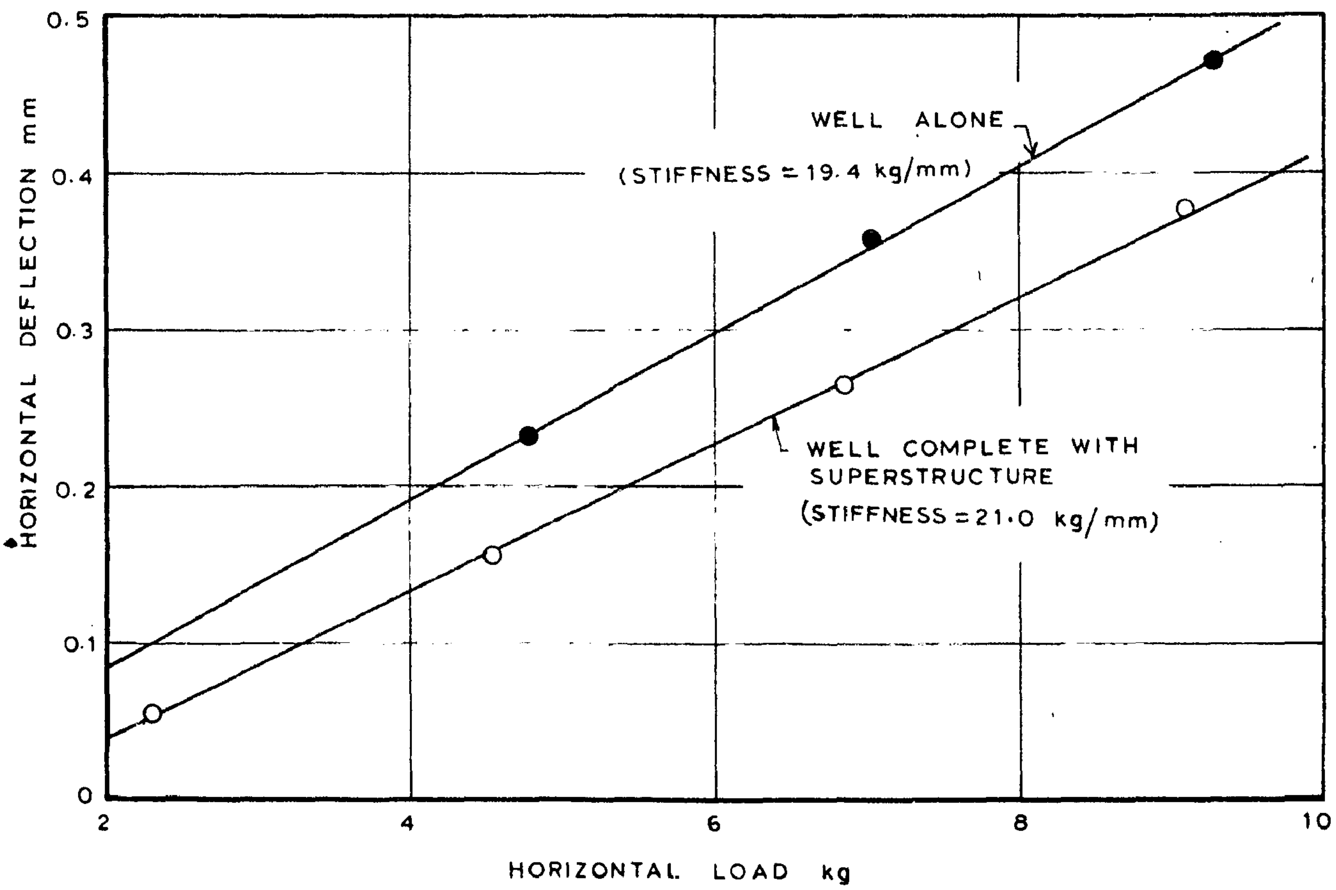

LOAD ALONG YY AXIS

FIG. 3.3 _ LOAD DEFLECTION DIAGRAM OF WELL MODEL FIXED AT BASE (Horizontal load at 10 mm below top of well mode

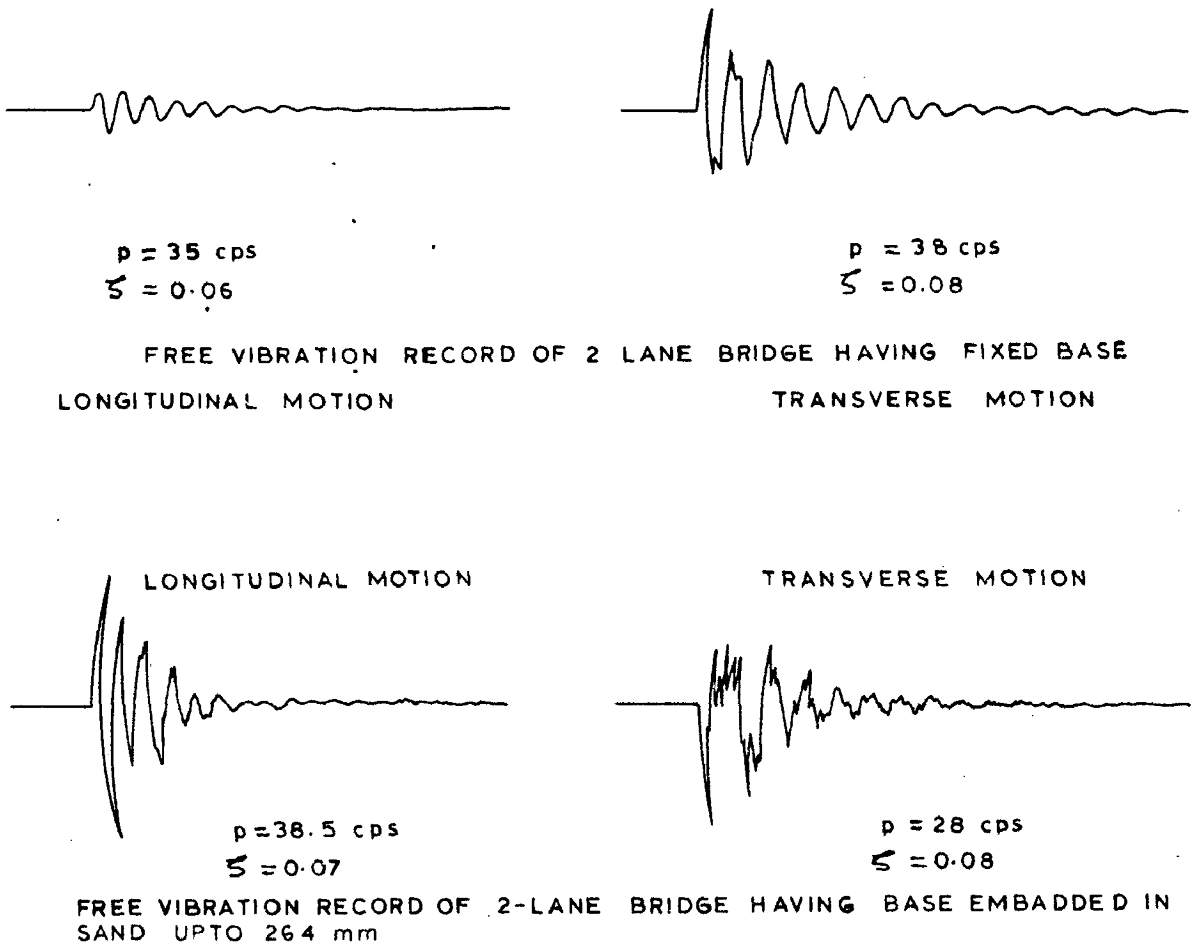

FIG. 3.5 _ FREE VIBRATION RECORD

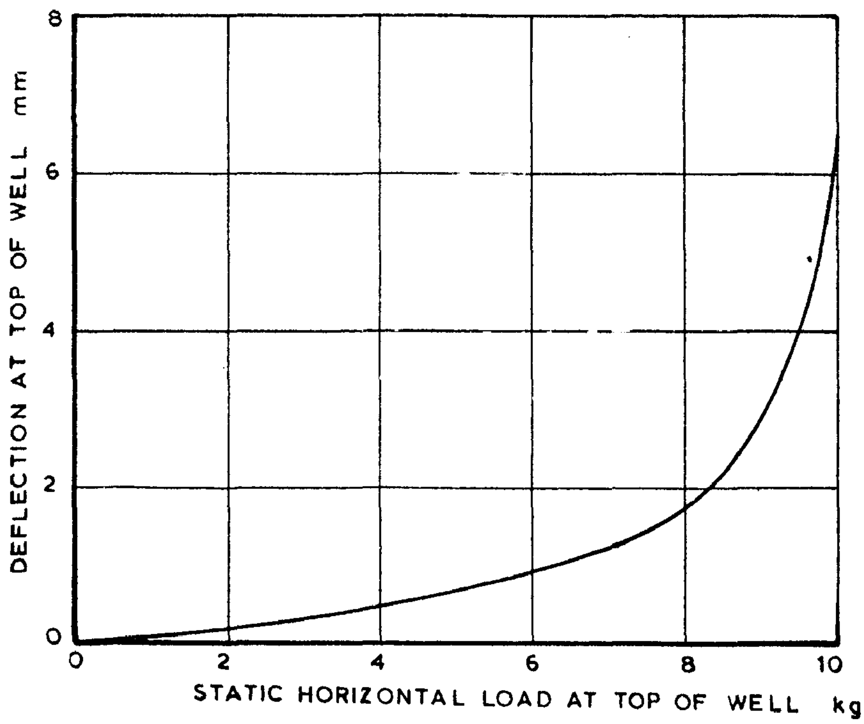

FIG.3.4 _ LOAD DEFLECTION DIAGRAM OF BRIDGE MODEL EMBEDDED IN SAND UPTO 264 mm AT THE BASE

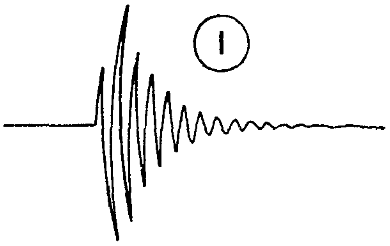

$p = 55.5$ c/s
$\zeta = 0{\cdot}09$

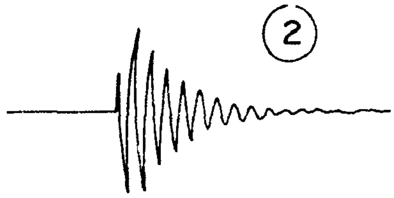

$p = 55.5$ c/s
$\zeta = 0{\cdot}07$

FREE VIBRATION RECORD OF WELL ALONE FIXED AT BASE

TRANSVERSE DIRECTION — LONGITUDINAL DIRECTION

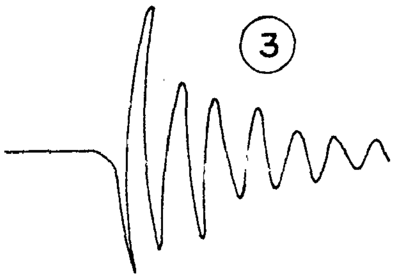

$p = 21.2$ c/s
$\zeta = 0{\cdot}08$

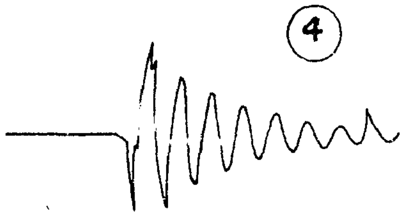

$p = 28$ c/s
$\zeta = 0{\cdot}06$

FREE VIBRATION RECORD OF 4-LANE BRIDGE
HAVING FIXED BASE

LONGITUDINAL DIRECTION — TRANSVERSE DIRECTION

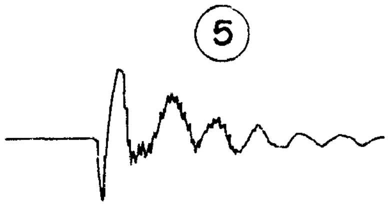

$p = 20$ c/s
$\zeta = 0{\cdot}083$

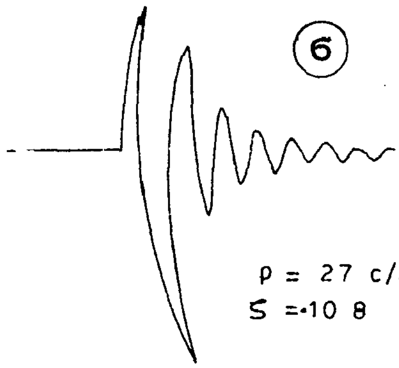

$p = 27$ c/s
ζ =·10 8

FREE VIBRATION RECORD OF 4-LANE BRIDGE
HAVING BASE EMBEDDED IN SAND UPTO SCOUR LEVEL

LONGITUDINAL DIRECTION — TRANSVERSE DIRECTION

FIG. 3.6_ FREE VIBRATION RECORDS

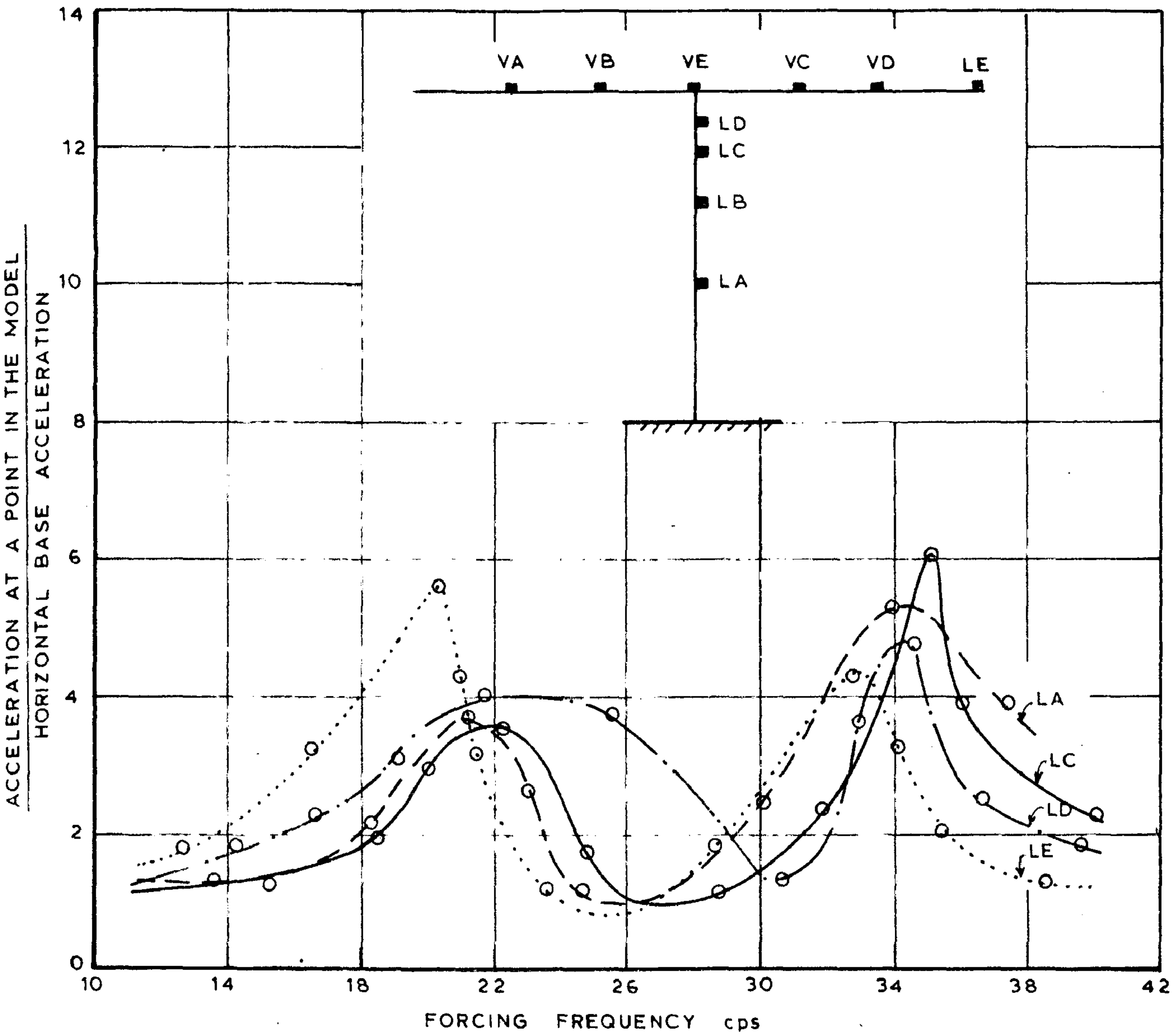

FIG. 3.7 _ RESONANCE CURVES FOR STEADY STATE TEST OF 2 LANE BRIDGE MODEL IN LONGITUDINAL DIRECTION WITH FIXED BASE

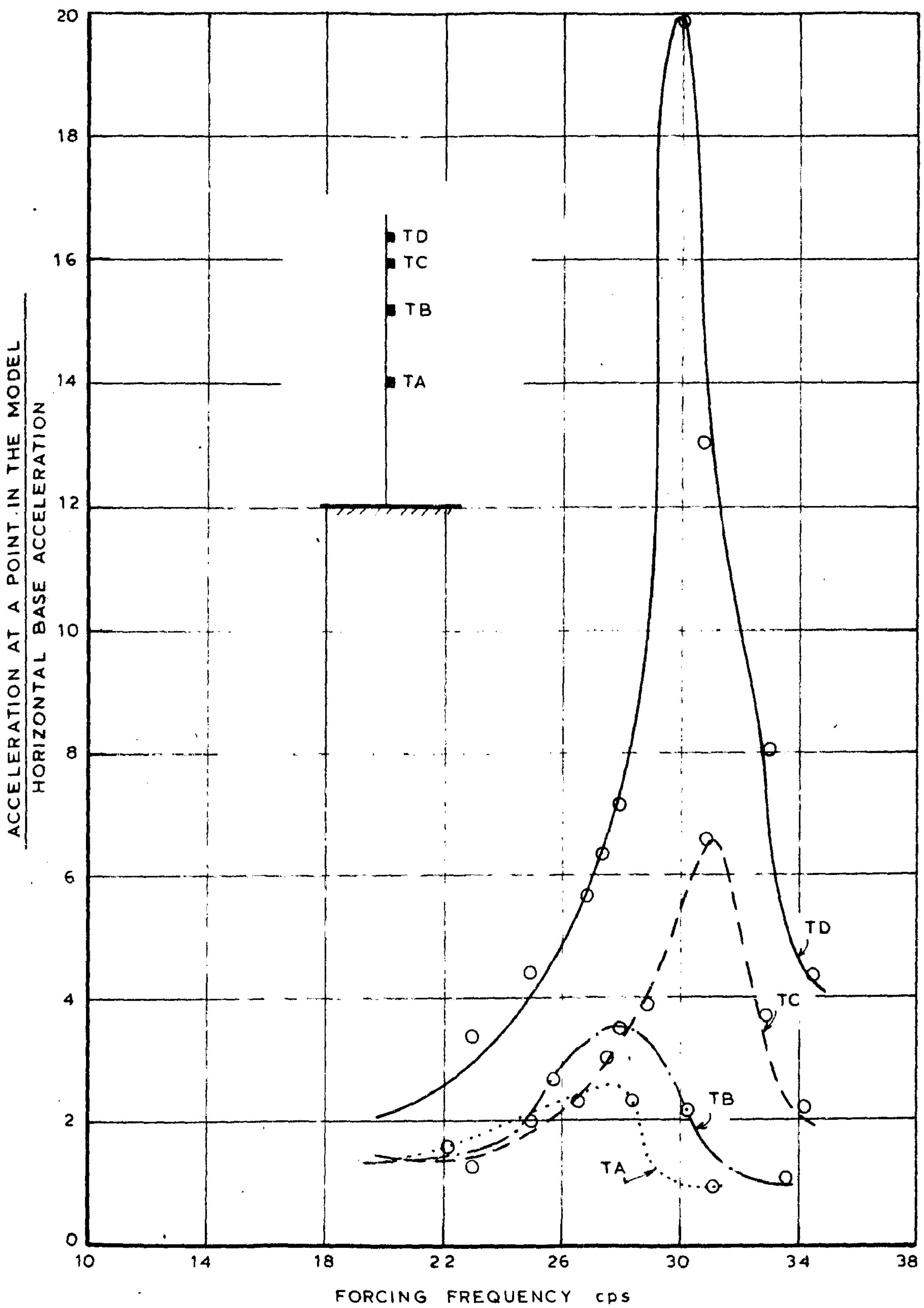

FIG. 3.8 _ RESONANCE CURVES FOR STEADY STATE TEST OF 2-LANE BRIDGE MODEL IN TRANSVERSE DIRECTION WITH FIXED BASE

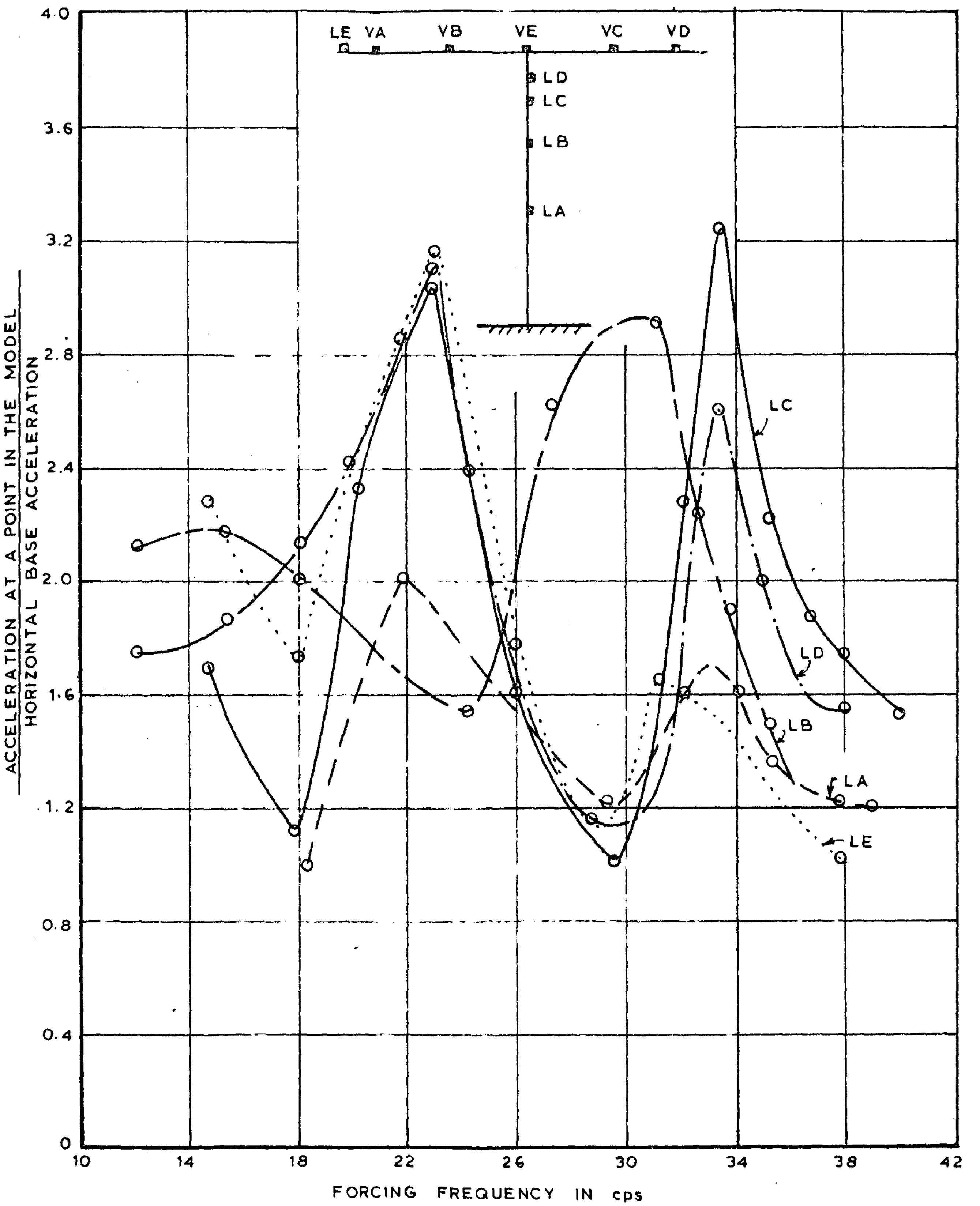

FIG. 3.9 _ RESONANCE CURVES FOR STEDY STATE TEST OF 2-LANE BRIDGE MODEL IN LONGITUDINAL DIRECTION WITH SAND UPTO SCOUR LEVEL

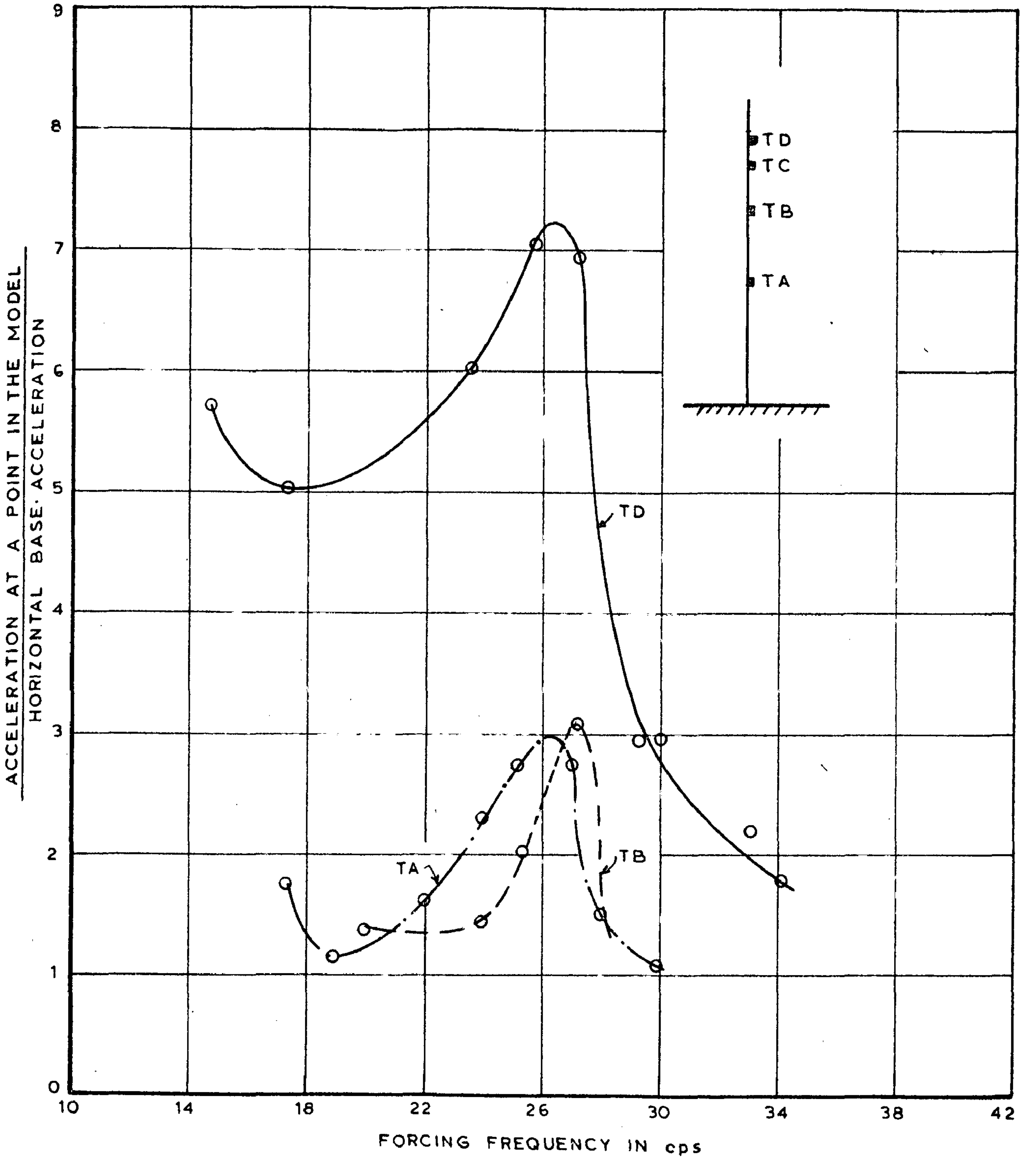

FIG. 3.10_ RESONANCE CURVES FOR STEDY STATE TEST OF 2-LANE BRIDGE MODEL IN TRANSVERSE DIRECTION WITH SAND UPTO SCOUR LEVEL

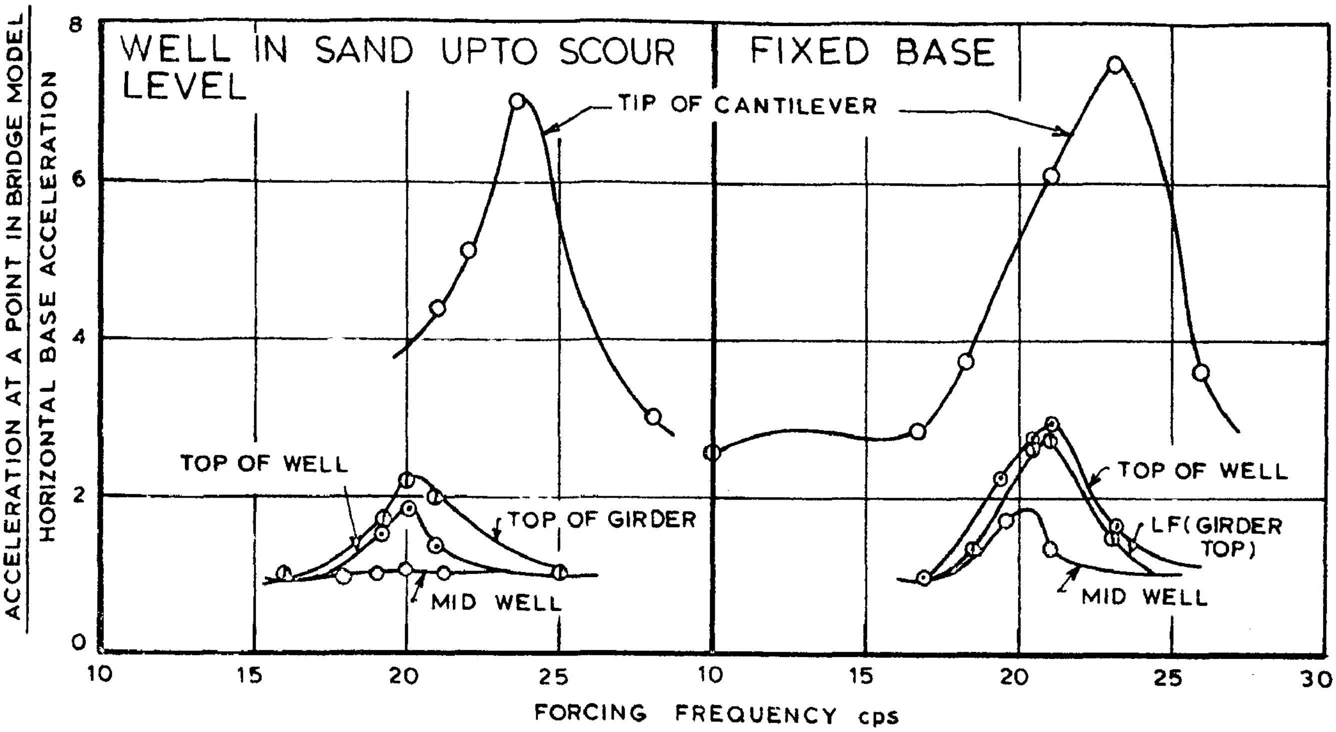

RESONANCE CURVES

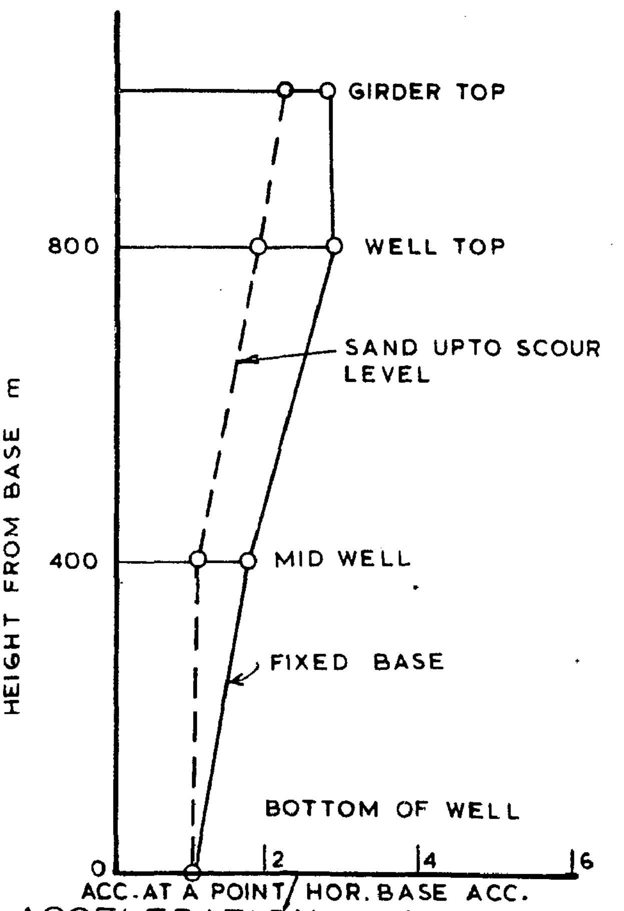

ACCELERATION DISTRIBUTION

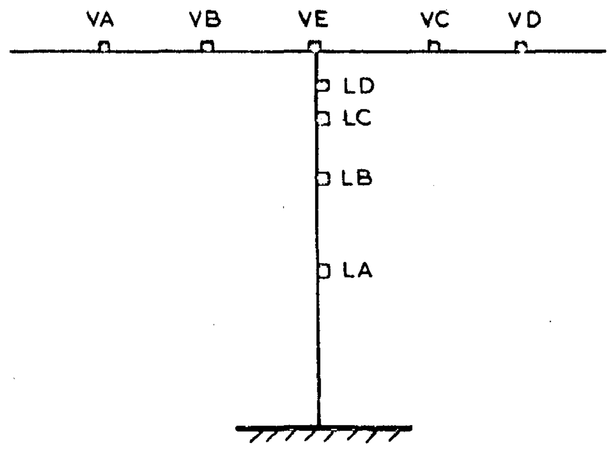

FIG. 3.11 – ACCELERATION DISTRIBUTION AND RESONANCE CURVES FOR STEADY STATE TEST OF 4-LANE BRIDGE MODEL IN LONGITUDINAL DIRECTION

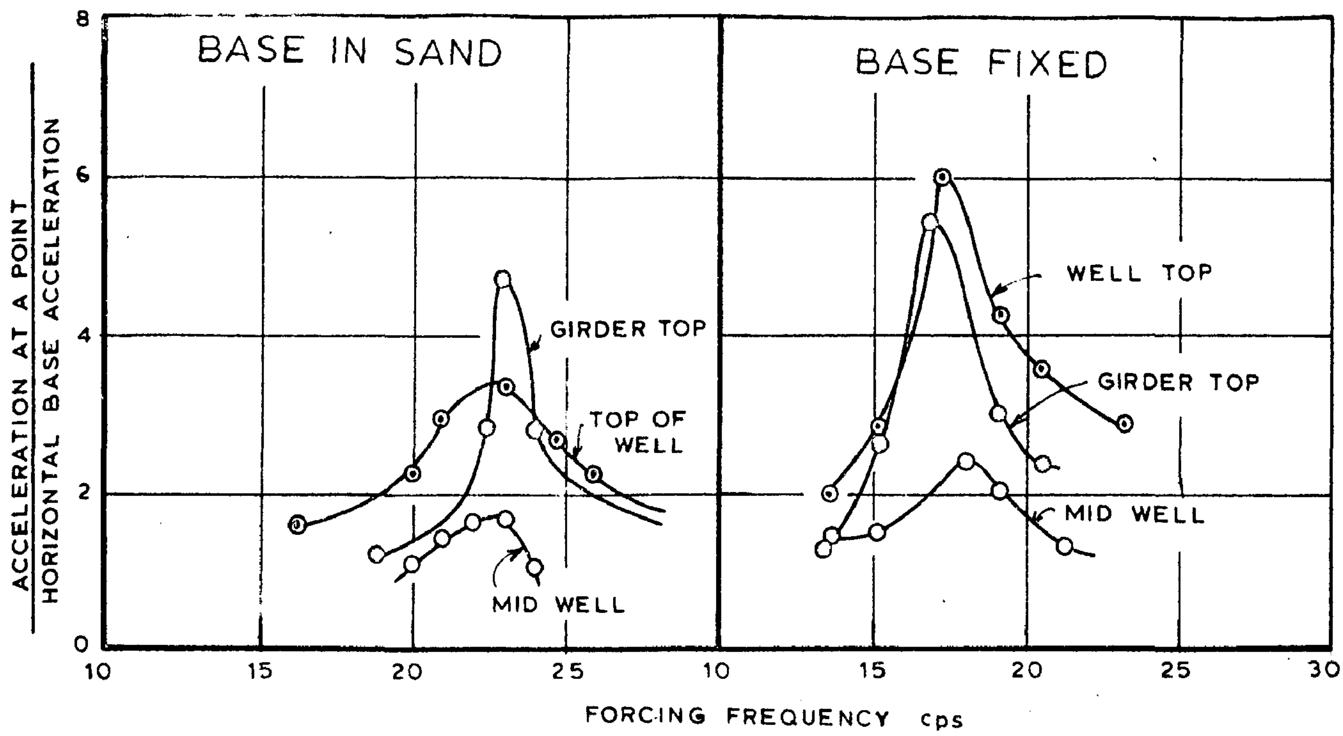

RESONANCE CURVES (TRANSVERSE MOTION)

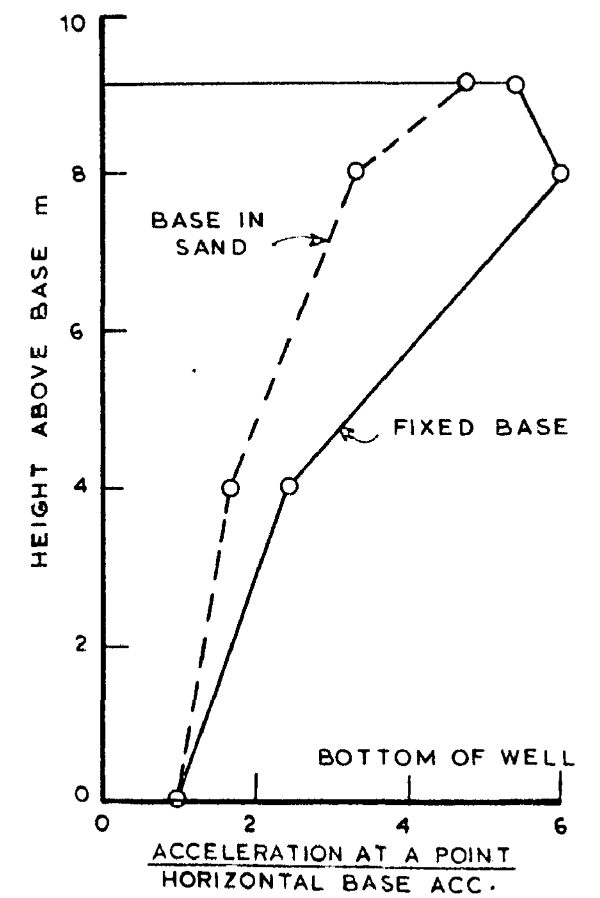

ACCELERATION DISTRIBUTION (TRAN. MOTION)

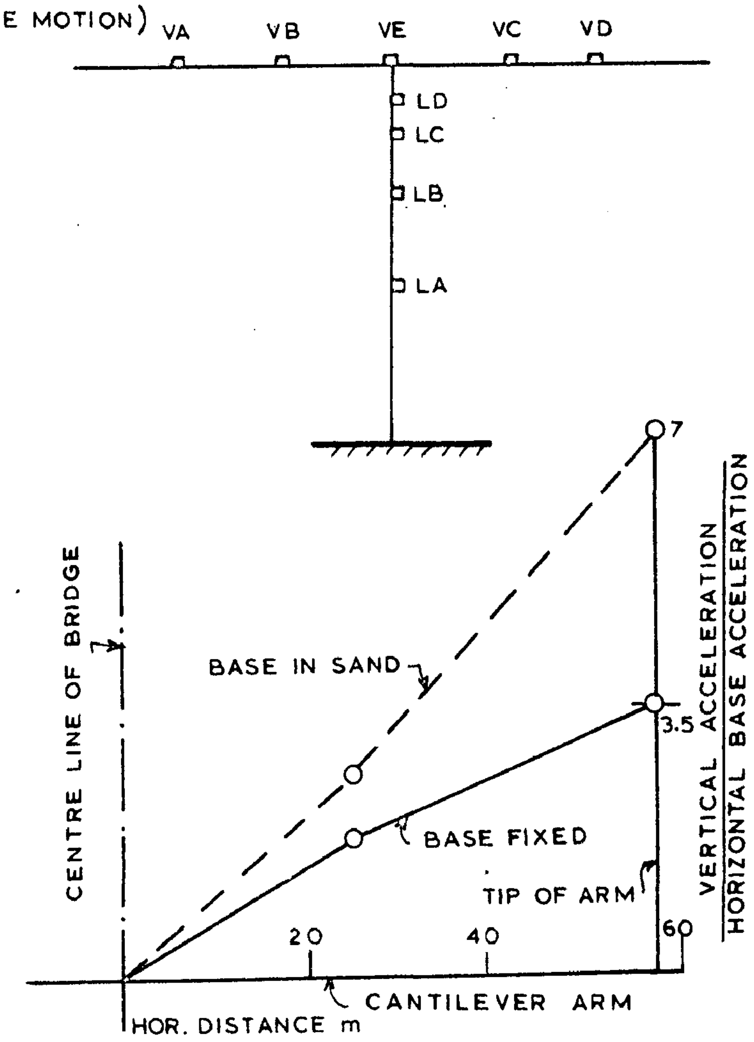

ACCELERATION DISTRIBUTION IN CANTILEVER ARM (LONG. MOTION)

FIG.3.12 – ACCELERATION DISTRIBUTION AND RESONANCE CURVES FOR STEADY STATE TEST OF 4-LANE BRIDGE MODEL

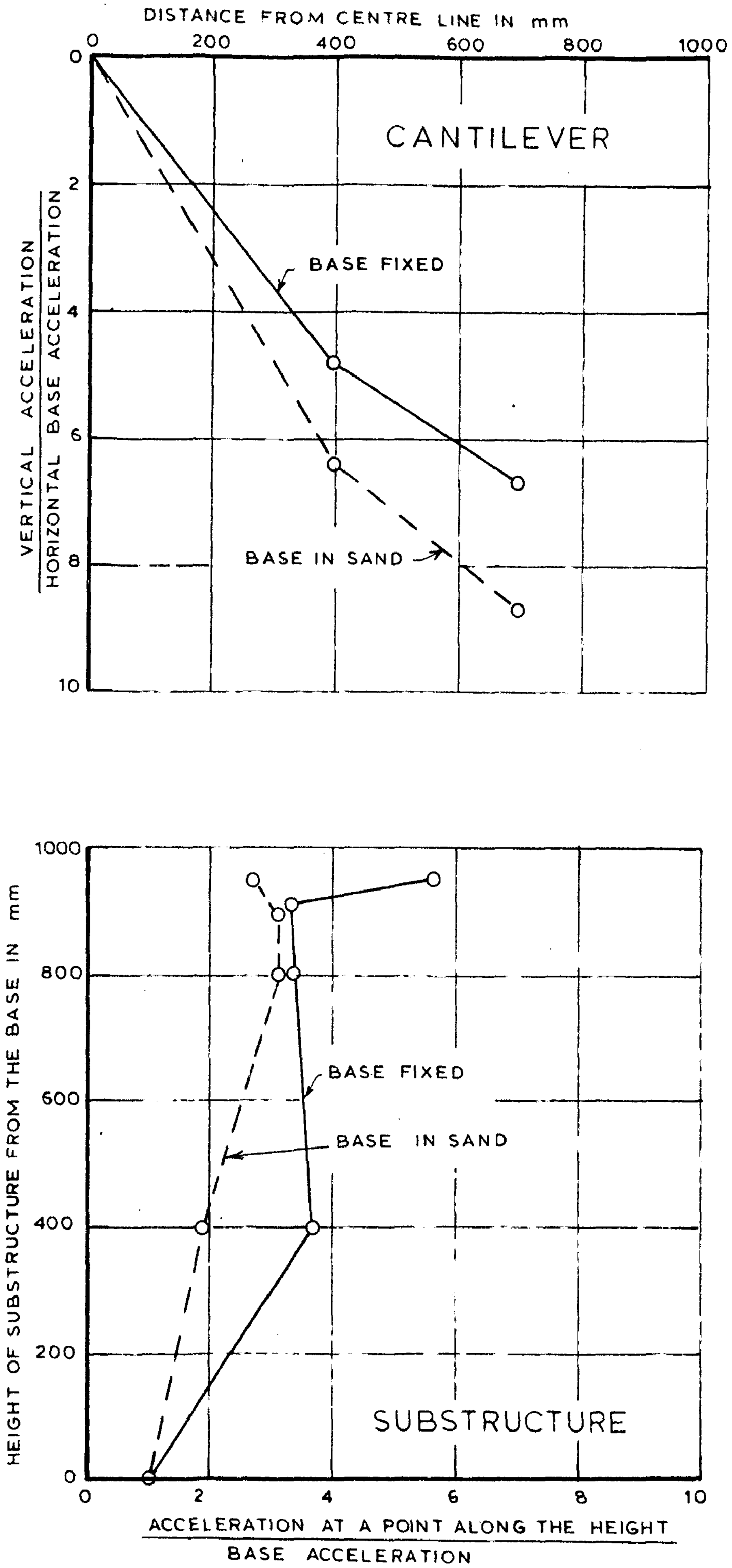

FIG. 3.13 – ACCELERATION DISTRIBUTION ALONG THE HEIGHT OF STRUCTURE AND LENGTH OF CANTILEVER ARM DUE TO STEADY STATE TEST OF 2-LANE BRIDGE IN HORIZONTAL DIRECTION (LONGITUDINAL)

CHAPTER 4

THEORETICAL INVESTIGATION AND RESULTS

4.1 General

Since substantial proportion of the mass of the bridge is distributed over the cantilever arms which undergoes horizontal as well as vertical displacement during longitudinal motion of the bridge, the usual method of bending - shear analysis applicable to stack like structure can not be used here. So Rayleigh's method has been employed to calculate fundamental natural frequency of the bridge model. Dynamic response of the prototype has been worked out for a typical earthquake motion.

4.2 Details of Analysis

(a) Static deflection of the well alone fixed at the base

For a cantilever deflection at the free end,

$$\delta = \frac{PL^3}{3EI} + \frac{\alpha_s PL}{GA}$$

where P is the applied transverse load at the end of the cantilever of length L.

G is the modulus of rigidity

α_s is the shape factor for shear defined as

$$\sigma_s = \frac{A}{I^2} \int_A \frac{Q^2}{b^2} \, dA$$

For a thin tube $\sigma_s = 2.0$

$$G = \frac{E}{2(1+\mu)} = \frac{E}{2(1+.36)}$$

Here $L = 790$ mm

$E = 226$ kg/mm²

$I = 20.8 \times 10^6$ mm⁴

$A = 9860$ mm²

Putting the above values

$$\frac{P}{\delta} = 26 \text{ kg per mm}$$

(b) Natural frequency of vibration of the well alone fixed at the base -

We have the well known relation

$$p_n = \frac{(r_n L)^2}{L^2} \sqrt{\frac{EIg}{A\rho}}$$

Where $r_n L = 1.875$ for cantilever

$E = 226$ kg/mm²

$I = 20.8 \times 10^6$ mm⁴

$A = 9860$ mm²

$g = 9810$ mm/sec²

$= 1.2$ gm/cc $= 1.2 \times 10^{-3}$ g/mm³

$L = 800$ mm

Substituting above values

$p_1 = 344$ radians/sec $= 54.7$ cps

(c) Natural frequency of the bridge model

To apply Rayleigh's method to calculate the first fundamental frequency in longitudinal direction, masses of the bridge model were lumped as shown in Fig. 4.1. Loads equal to weights of various masses were applied on the mass points as shown in the figure. Forces and resulting deflections are given in Table 4.1 and 4.2. For transverse vibration the mass of the entire superstructure was lumped at the centre of gravity and is denoted by mass 8.

TABLE 4.1

HORIZONTAL DEFLECTION OF THE MODEL IN TRANSVERSE DIRECTION DUE TO WEIGHTS OF MASSES 1 TO 8 APPLIED HORIZONTALLY

	4 Lane Bridge			2 Lane Bridge		
Mass No.	Force in gm	Nature	Deflection H_i (mm)	Force in gm	Nature	Deflection h_i (mm)
1	1860	Horiz.	.002	1860	Horiz.	.002
2	1860	"	.034	1860	"	.028
3	1860	"	.086	1860	"	.075
4	1860	"	.16	1860	"	.139
5	1860	"	.22	1860	"	.20
6	280	"	.24	280	"	.21
7	342	"	.296	171	"	.247
8	3278	"	.318	1750	"	.288

TABLE 4.2

DEFLECTION OF THE MODEL IN LONGITUDINAL DIRECTION
DUE TO WEIGHTS OF MASSES AS SHOWN IN FIGURE 4.1

Mass No.	4 Lane Bridge				2 Lane Bridge			
	Force in gm	Nature	Deflection		Force in gm	Nature	Deflection	
			h_i	v_i			h_i	v_i
1	1860	Horiz.	.002	-	1860	Horiz.	.002	-
2	1860	"	.038	-	1860	"	.029	-
3	1860	"	.116	-	1860	"	.084	-
4	1860	"	.217	-	1860	"	.156	-
5	1860	"	.325	-	1860	"	.228	-
6	280	"	.356	-	280	"	.248	-
7	342	"	.430	-	171	"	.297	-
8	3278	"	.508	-	1750	"	.340	-
9								
28	66	Vert.	.508	.837	33	Vert.	.340	.50
29	165	"	"	.754	93	"	"	.450
30	176	"	"	.639	98	"	"	.392
31	195	"	"	.498	108	"	"	.307
32	205	"	"	.378	113	"	"	.230
33	227	"	"	.161	124	"	"	.159
34	236	"	"	.140	127	"	"	.09
35	124	"	"	.060	70	"	"	.036
36	124	"	"	-.060	70	"	"	-.036
37	236	"	"	-.140	127	"	"	-.09
38	227	"	"	-.161	124	"	"	-.159
39	205	"	"	-.378	113	"	"	-.230
40	195	"	"	-.498	108	"	"	-.307
41	176	"	"	-.639	98	"	"	-.392
42	165	"	"	-.754	93	"	"	-.450
43	66	"	"	-.837	33	"	"	-.500

Note : 1. h_i means the horizontal deflection of mass i
v_i means the vertical deflection of mass i
2. vertical deflection downward is taken positive.

Here only the fundamental mode of vibration have-been has been considered. The result of analysis is given below in table 4.3.

TABLE 4.3

FUNDAMENTAL FREQUENCY AND MODE PARTICIPATION FACTOR FOR BRIDGE MODEL FIXED AT BASE

Description	p for model cps	p for prototype cps	T for prototype sec	C_r
4 Lane Bridge				
Long.	20.4	.392	2.55	1.73
Trans.	31.4	.582	1.72	3.96
2 Lane bridge				
Long.	28.1	.52	1.92	3.2
Trans.	34.8	.555	1.8	4.9

Note : The natural frequency of the prototype has been calculated from the relation $p_m/p_p = 54$ derived earlier.

Ground Motion Chosen for Response Calculation

The displacement spectra of the ElCentro earthquake May 18, 1940 N-S component reduced by a factor .349 has been adopted for response calculation. The values of spectral displacements for different time periods are given in table 4.4.

Natural frequency is calculated from the relation

$$p^2 = g \frac{\sum W_i\ h_i + W_i\ V_i}{\sum W_i\ (h_i^2 + v_i^2)}$$

Where W_i is the weight of mass i

Modal Analysis

The response in the rth mode of vibration due to earthquake motion can be obtained from

$$X_r = C_r\ x_r\ S_{dr}$$

where

X_r = Dynamic response desired which may be deflection, bending moment, shear or any other quantity.

C_r = Mode participation factor

$$= \frac{\sum_{i=1}^{N} m_i\ y_{ir}}{\sum_{i=1}^{N} m_i\ y^2_{ir}}$$

x_r = Model values of deflection, bending moment or any other quantity under consideration.

y_{ir} = horizontal displacement of mass m_i at i in rth mode.

N = Number of masses

S_{dr} = Spectral displacement in rth mode of vibration.

Here only the fundamental mode of vibration ~~have been~~ has been considered. The result of analysis is given below in table 4.3.

TABLE 4.3

FUNDAMENTAL FREQUENCY AND MODE PARTICIPATION FACTOR FOR BRIDGE MODEL FIXED AT BASE

Description	p for model cps	p for prototype cps	T for prototype sec	C_r
4 Lane Bridge				
Long.	20.4	.392	2.55	1.73
Trans.	31.4	.582	1.72	3.96
2 Lane bridge				
Long.	28.1	.52	1.92	3.2
Trans.	34.8	.555	1.8	4.9

Note : The natural frequency of the prototype has been calculated from the relation $p_m/p_p = 54$ derived earlier.

Ground Motion Chosen for Response Calculation

The displacement spectra of the ElCentro earthquake May 18, 1940 N-S component reduced by a factor .349 has been adapted for response calculation. The values of spectral displacements for different time periods are given in table 4.4.

TABLE 4.4

SPECTRAL DISPLACEMENTS FOR SELECTED EARTHQUAKE MOTION

Point No.	Time period (sec)	Sd (m) for 5% Damping
1	0.10	0.00050362
2	0.12	0.00074086
3	0.14	0.00109210
4	0.16	0.00182597
5	0.18	0.00259741
6	0.20	0.00350360
7	0.25	0.00430809
8	0.30	0.00588782
9	0.35	0.00923417
10	0.40	0.01190000
11	0.45	0.01400000
12	0.50	0.01650000
13	0.55	0.01850000
14	0.60	0.02100000
15	0.65	0.02300000
16	0.70	0.02500000
17	0.75	0.02700000
18	0.80	0.02900000
19	0.85	0.03100000
20	0.90	0.03300000
21	0.95	0.03400000
22	1.00	0.03550000
23	1.20	0.03900000
24	1.40	0.04150000
25	1.60	0.04300000
26	1.80	0.04600000
27	2.00	0.05676103
28	2.20	0.08963100
29	2.40	0.12170362
30	2.50	0.13320768
31	3.00	0.13736827

Dynamic response calculated with the above values are given in tables4.5 and 4.6

TABLE 4.5

DYNAMIC RESPONSE OF THE PROTOTYPE BRIDGE
TO SELECTED EARTHQUAKE MOTION (4 LANE BRIDGE)

Height from base in m	Longitudinal Motion			Transverse Motion		
	Bending moment tm	Shear force t	deflection mm	Bending moment tm	Shear force t	deflection m
0	53963	675.2	0	43492	668.7	0
6.71	49468	675.2	.46	38492	668.7	.4
20.04	40458	674.4	8.7	30095	667.5	6.8
33.40	31588	659.4	26.5	21440	647.8	17.2
46.70	23482	614.1	50.0	13422	597.8	32.0
60.03	16437	529.1	74.0	6756	504.8	44.0
67.2	13532	402.1	81.4	4018	376.8	48.0
71.5	11868	381	98.0	2500	355.8	60.0
79.2	9188	350	116	0	324	63

Distance on cantilever from centre m			h_i	v_i
0	4594	114.8	116	0
5	4024	114.8	"	13.5
11.6	3264	113.2	"	31.6
19.93	2326	106.2	"	36.0
28.26	1566	98.5	"	85.0
36.6	883	82.0	"	113.0
44.93	363	61.5	"	144
53.26	54	37.7	"	170.0
57.93	0	11.50	"	189

TABLE 4.6

DYNAMIC RESPONSE OF THE PROTOTYPE BRIDGE
TO SELECTED EARTHQUAKE MOTION (2 LANE BRIDGE)

Height from base in m	Longitudinal Motion: Bending moment (tm)	Longitudinal Motion: Shear force (t)	Longitudinal Motion: deflection (m)	Transverse Motion: Bending moment (tm)	Transverse Motion: Shear force (t)	Transverse Motion: deflection (m)
0	22682	422	0	37015	609	0
6.77	20484	422	.32	32902	609	.4
20.04	16212	420	4.8	24895	607	6.4
33.40	12001	410	13.8	17040	585	17.0
46.70	8346	280	25.6	10080	526	31 .0
60.08	5403	223	37.4	4487	416	45.0
67.2	4493	140	41.0	2648	257	47.0
71.5	3860	126	49.0	1640	232	56.0
79.2	2960	116	56.0	0	214	65.0

Distance on cantilever from centre m			h_i	v_i
0	1480	37.9	56.0	0
5	1286	37.9	"	6
11.6	1044	37.4	"	15
19.93	751	35.2	"	26
28.26	490	31.3	"	38
36.6	271	26.2	"	50
44.93	112	19.1	"	64
53.26	16	11.6	"	75
57.93	0	2.3	"	82

The dynamic response has been plotted in figures 4.2 and 4.3.

4.3 Comparison of Experimental and Theoretical Results

Stiffness of the well alone having fixed base with respect to a horizontal load applied 10 mm below the top of well was measured to be 19.4 kg/mm but theoretically it was found to be 26 kg/mm. Thus it appear that the fixity of the base was not perfect.

The natural frequency of the bridge model fixed at base obtained from experiments and the corresponding resonant frequency obtained from theoretical analysis are tabulated below for comparison.

TABLE 4.7

FUNDAMENTAL NATURAL FREQUENCIES OF BRIDGE MODEL

Description	Experimental resonant frequency cps	Theoretical cps
4 Lane Bridge		
Long.	22.2	20.4
Trans.	17.0	31.4
2 Lane Bridge		
Long.	21.0	28.1
Trans.	27.0	34.8

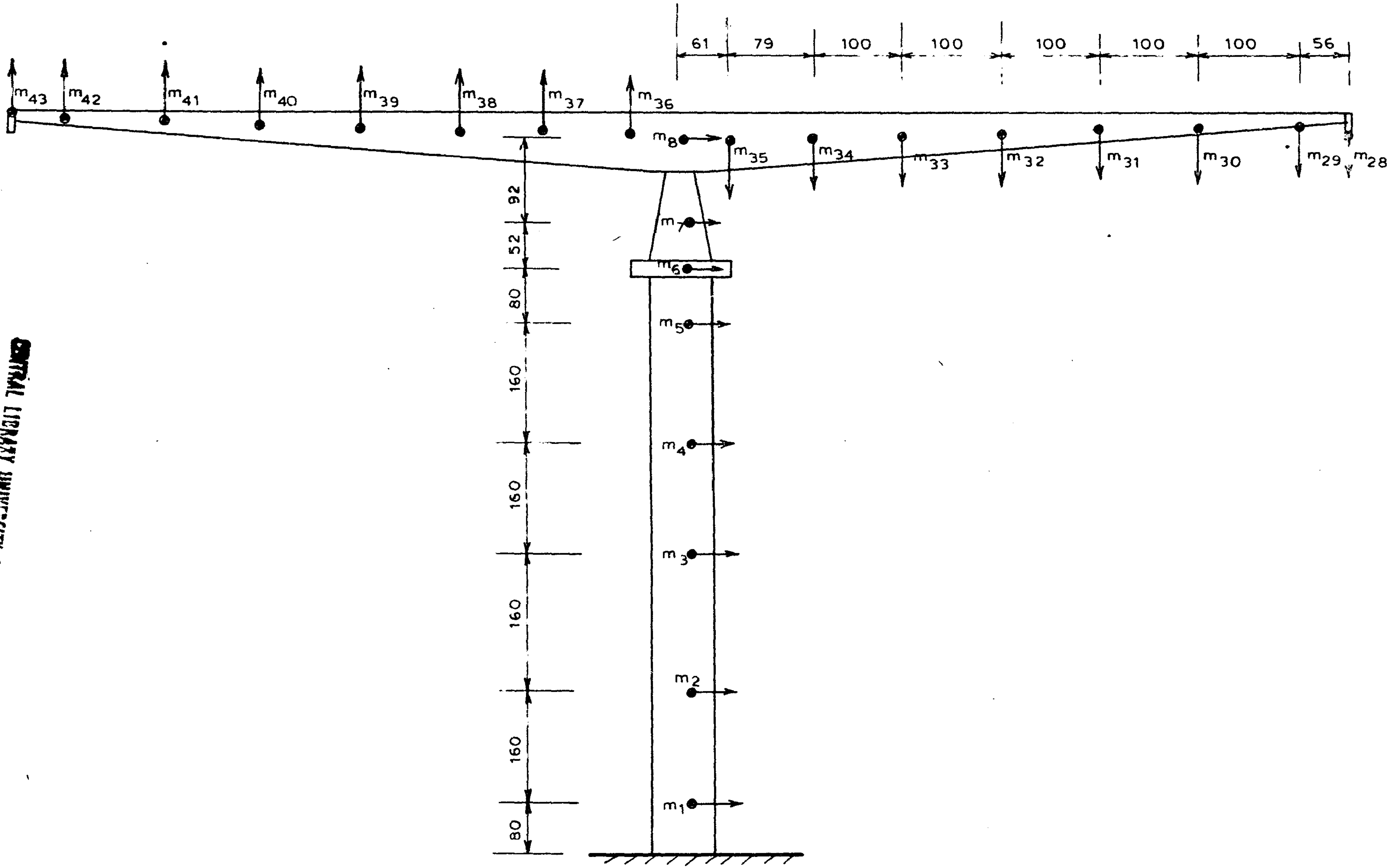

FIG. 4.1 _ LUMPED MASS SYSTEM OF PERSPEX BRIDGE MODEL
(LONGITUDINAL DIRECTION)

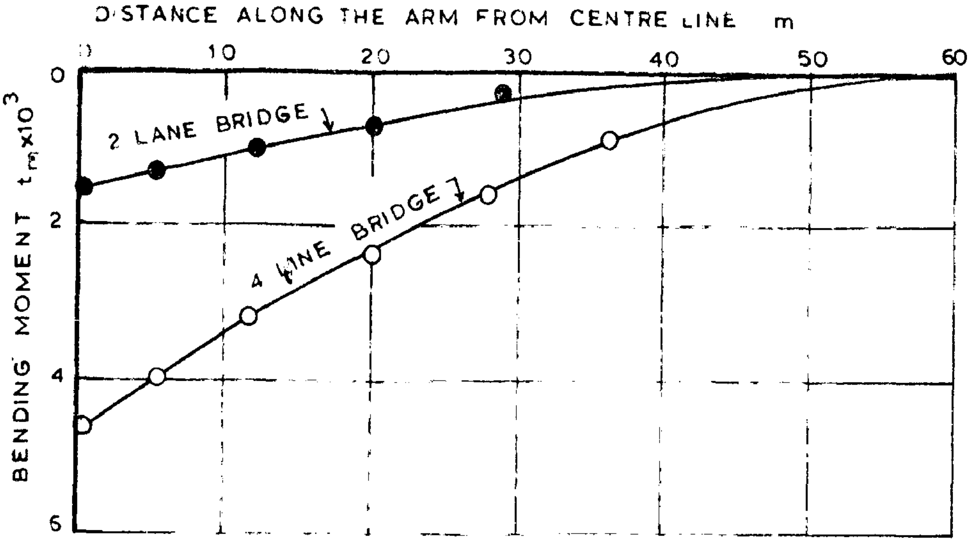

DYNAMIC MOMENT IN CANTILEVER ARM

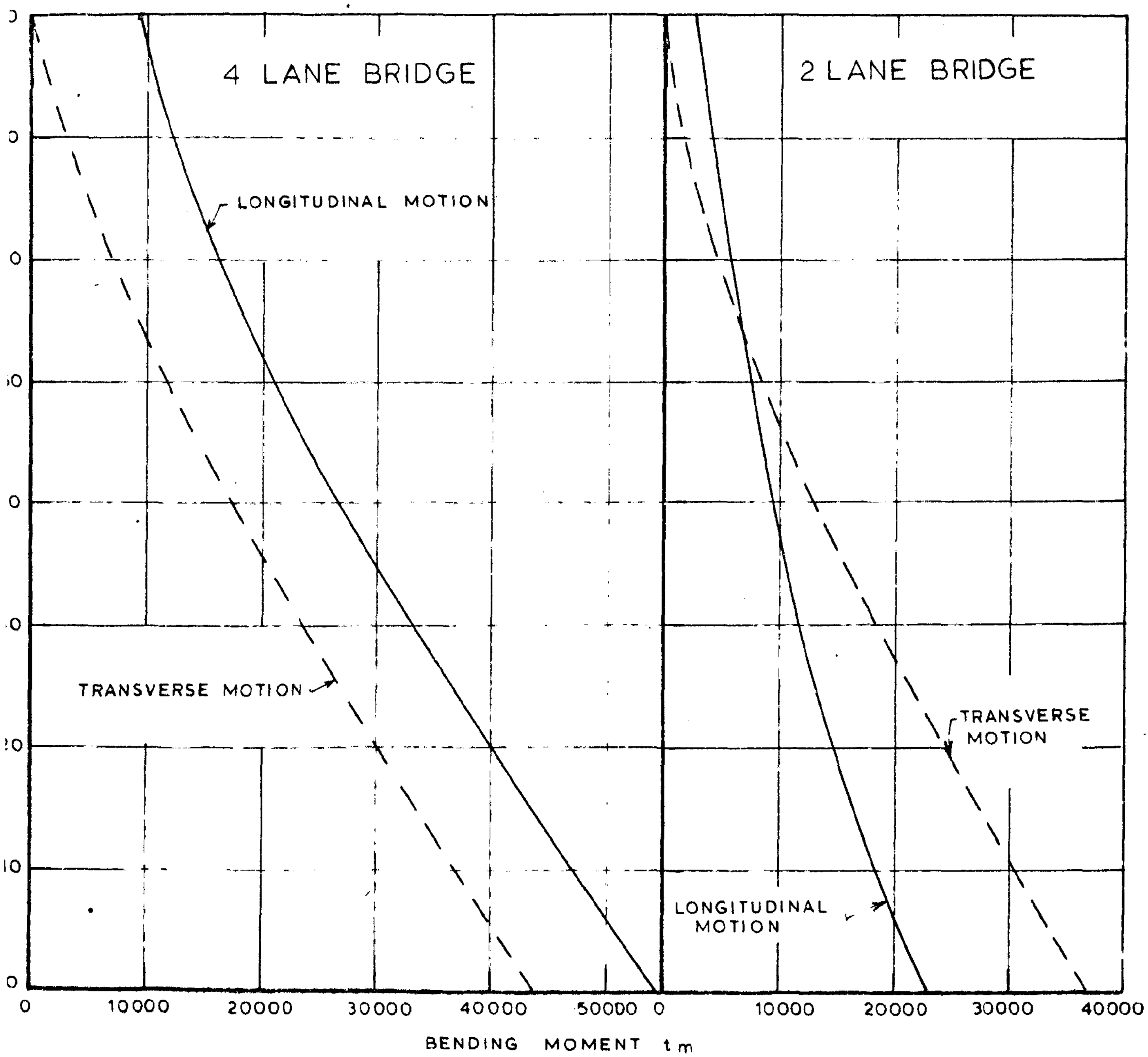

FIG 4 2 . DYNAMIC MOMENT IN WELL AND PIER UNDER REDUCED EL CENTRO EARTHQUAKE MAY 18, 1940

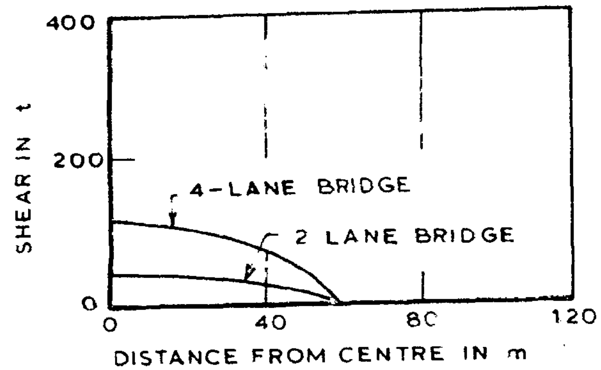

SHEAR IN CANTILEVER ARM DURING LONGITUDINAL MOTION

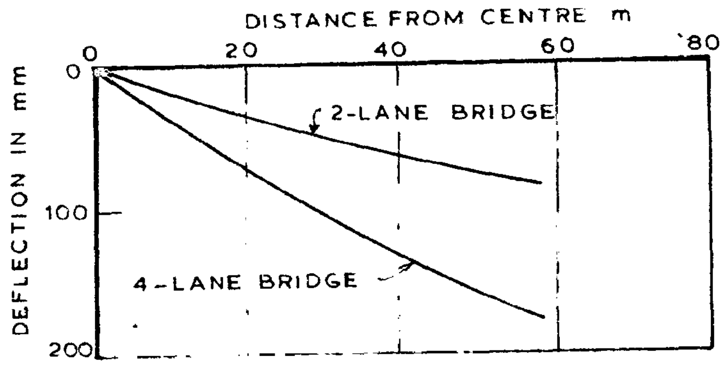

VERTICAL DEFLECTION OF CANTILEVER ARM DURING LONGITUDINAL MOTION

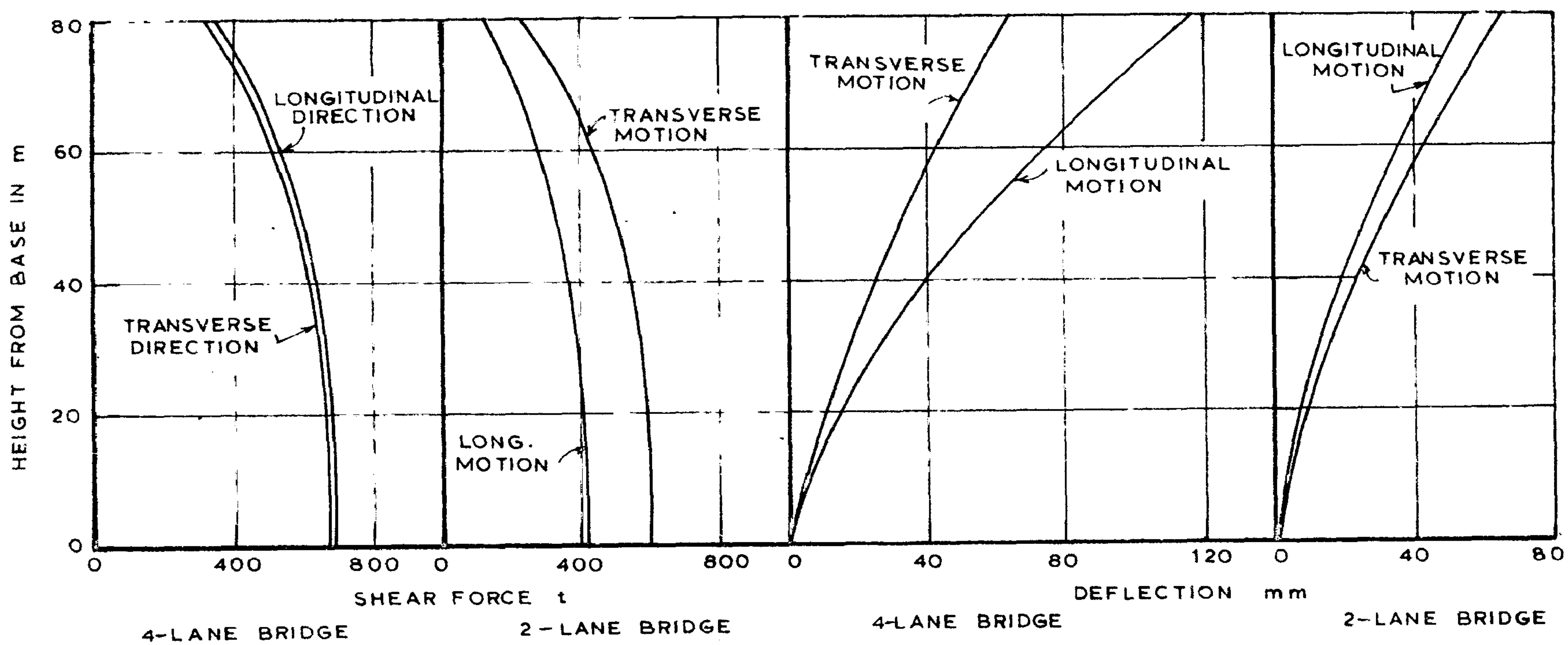

SHEAR IN SUBSTRUCTURE

DEFLECTION OF SUBSTRUCTURE

FIG. 4.3 _ DYNAMIC SHEAR AND DEFLECTION IN PROTOTYPE BRIDGE WITH FIXED BASE

CHAPTER 5

CONCLUSIONS AND RECOMMENDATIONS

1. The effect of bending of cantilever arms on the dynamic response of bridge during motion in the longitudinal direction is substantial. If the design of such a bridge is done by the uniform seismic coefficient method considering the entire superstructure lumped at its centre of gravity. There will be no dynamic moment in the cantilever arm and the pier at the junction. But the foregoing dynamic analysis indicates that the dynamic moment even for a substantially reduced accelerogram (0.349 of the displacement spectra of the ElCentro Earthquake of May 18, 1940, N-S component) in each of the cantilever arm is 11.3 % of dead load moment and the dynamic moment in the pker at the junction will be numerically twice that amount.

2. Ratio of horizontal acceleration at a point to the base acceleration along the substructure in case of longitudinal motion is less when the well is embedded in sand than when it is fixed at the base level, but along the arm reverse takes place. The ratio of vertical acceleration to the horizontal base acceleration on the cantilever arm is higher when the base is in sand.

3. The horizontal deflection of superstructure in 4 lane prototype bridge is seen to be 116 mm. The deflection of the cantilever arm of the same is 189 mm at the tip. But for 2 lane bridge the horizontal deflection is 56 mm but the vertical deflection is 65 mm.

4. The weight of superstructure in the 4 lane bridge is nearly double of that of 2 lane bridge but the dynamic moment at the junction of the cantilever arm with the pier is nearly thrice in case of longitudinal motion.

5. Embedment in soil increases the dynamic response of the cantilever arms in areas where vertical vibration of ground have been recorded. This aspect need utmost consideration.

RECOMMENDATIONS

It is recommended that the different soil conditions may be considered at the base. The vertical vibration is important for such bridges and hence due emphasis should be given to make cantilever arm strong against possible vertical vibration. Dynamic analysis should be perfomed for design of such bridges located in earthquake zones.

REFERENCES

1. Iwasaki, T., Penzien, J, Clough, R., "Literature Survey Seismic Effects on Highway Bridges", EERC 71-11, Earthquake Engineering Research Centre, University of California, Berkley, November 1972.

2. Tseng, W.S., Penzien, J., "Analytical Investigations of the Seismic Response of Long Multiple Span Highway Bridges", EERC 73-12, Earthquake Engineering Research Centre, University of California, Berkley, June 1973.

3. The Bihar Nepal Earthquake of 1934. Memoirs of the Geophysical Survey of India, Volume 73, 1939.

4. "I.S.: 1893-1970", Criteria of Earthquake Resistant Design of Structures", Indian Standards Institution.

5. Krishna, J., Arya, A.S., and Thakkar, S.K., "Dynamic Analysis and Model Studies of Ganga Bridge at Allahabad for Earthquake Motions", Earthquake Engineering Studies, School of Research and Training in Earthquake Engineering, University of Roorkee, Roorkee, Oct. 1969.

6. Charleson, A.W., "The Dynamic Behaviour of Bridge Substructures", M.E. Thesis, University of Canterbury, New Zealand.

7. Newmark, N.M., and Rosenblueth, Emilio, "Fundamentals of Earthquake Engineering", Prentice Hall International 1971.

8. Okamoto Shunzo, "Introduction to Earthquake Engineering", University of Tokyo, Press 1973.

9. Timoshenko, S.P., "Vibration Problems in Engineering", D. Van Nostrand Company, Inc. Princeton, New Jersey, New York.

10. Timoshenko, S.P., and Gere, J.M., "Mechanics of Materials", Van Nostrand Reinhold Company, 1973.

11. Komendant, A.E., "Contemporary Concrete Structures", Mcgraw Hill Book Company 1970.

12. Roll, F., "Materials for Structural Models", Journal of of Strutural Division, ASCE (June 1968).

13. "Earthquake Resistant Design for Civil Engineering Structures, Earth Structures and Foundations in Japan", Compiled by Japan Society of Civil Engineers, 1964.

14. Krishna, J., "Basic Principles Underlying Seismic Design of Bridges", Third Symposium on Earthquake Engineering, University of Roorkee, November 1966.